NASA Technical Memorandum 72661

(NASA-TM-72661) SPACE SHUTTLE ORBITER TRIMMED CENTER-OF-GRAVITY EXTENSION STUDY. VOLUME 3: IMPACT OF RETROFITS FOR CENTER-OF-GRAVITY EXTENSION ON ORBITER THERMAL-PROTECTION SYSTEM Interim Technical

N79-20343

G3/34 Unclas 19459

SPACE SHUTTLE ORBITER TRIMMED CENTER-OF-GRAVITY EXTENSION STUDY

VOLUME III - IMPACT OF RETROFITS FOR CENTER-OF-GRAVITY EXTENSION ON ORBITER THERMAL PROTECTION SYSTEM

James C. Dunavant

February 1979

National Aeronautics and Space Administration

Langley Research Center
Hampton, Virginia 23665

SPACE SHUTTLE ORBITER TRIMMED CENTER-OF-GRAVITY EXTENSION STUDY VOLUME III - IMPACT OF RETROFITS FOR CENTER-OF-GRAVITY EXTENSION ON ORBITER THERMAL PROTECTION SYSTEM

James C. Dunavant
Langley Research Center

SUMMARY

Heat-transfer studies were conducted at Mach 10.3 on Space Shuttle Orbiter models, with the S-2 fillet and C-4 canard retrofit moldlines, which were generated in aerodynamic and system design studies to increase the allowable c.g. range of the orbiter. The heat-transfer results indicated that the lower surface heating was not significantly altered by the addition of the retrofits to the orbiter configuration nor did the additions adversely affect boundary-layer transition. Areas of orbiter most strongly affected were the sides where a shear layer which separated along the wing leading edge impinged. The area of impingement was, in general, larger for the baseline orbiter and C-4 canard configurations than the S-2 fillet configuration. Analytical studies of the heating effects on the Thermal Protection System (TPS) were made which indicated that scar weight on the orbiter sides due to all allowances for retrofits of the S-2 fillet and C-4 canard is small (less than about 90 kg (200 lbs) in comparison to the total weight of the retrofit).

INTRODUCTION

The longitudinal center-of-gravity range of the Space Shuttle Orbiter for trimmed flight during entry, approach, and landing is quite limited. This puts a considerable constraint on the allowable mass distribution of shuttle payloads. In an effort to extend the orbiter center-of-gravity envelope, a study was undertaken at the Langley Research Center into the feasibility of developing simple, "bolt-on" modifications. Modifications which were studied included changes in the fuselage nose shape and wing-fillet planform, and the addition of fixed canard surfaces. System-design analyses were undertaken to determine the weight penalties. Aerodynamic-heating tests and analyses provided information on the impact of the modifications on TPS requirements. Wind-tunnel force and moment tests were conducted across the speed range to assess the effectiveness of the modifications in extending the center-of-gravity envelope and the influence of the modifications on flight characteristics. Transonic and hypersonic aerodynamic characteristics of the modifications are presented in references 1 through 3 and system-design studies in reference 4. This report presents the results of the heat-transfer tests and analyses of the impact of the heating to the modified configurations on the shuttle orbiter TPS.

Two of the more promising configurations selected on the basis of the aerodynamic and design studies were investigated in the aerodynamic-heating studies. These two configurations are the extended fillet-strake (designated the S-2 fillet) and the fixed canard (designated the C-4 canard). Either of these two modifications provided sufficient forward c.g. control power at the critical Mach numbers (4 to 6) to trim expected sortie payloads. Wind-tunnel force and

moment tests conducted after the design studies and heat-transfer tests indicated the canard could be reduced in size to about 65 percent of its planform area. Although the canard of the heat-transfer studies is larger than necessary, the heat-transfer results should be representative since the leading-edge juncture and sweep of the smaller canard would be the same.

In the present study, heat-transfer tests were made of 0.01-scale models of the 140 A/B shuttle orbiter with the S-2 fillet and C-4 canard modifications. The baseline (no modifications) 140 A/B orbiter was also tested for comparison. The tests were performed in the Continuous Flow Hypersonic Tunnel at the Langley Research Center. The free-stream Mach number was 10.3 and the Reynolds numbers were 3.3 and 6.6 x 10^6 per meter (1.0 and 2.0 x 10^6 per foot).

SYMBOLS

Values are given in both SI and U.S. Customary Units. The measurements and calculations were made in U.S. Customary Units.

A	area
b	local span
h	heat-transfer coefficient, $\dot{q}/T_{aw}-T_w$
h_{ref}	heat-transfer coefficient to scaled 0.3048-m (1-foot) radius sphere
L	model length (from nose to trailing edge of body flap)
M	Mach number
r	radius
Re	Reynolds number
Re_θ	Reynolds number based on momentum thickness
$\dot{q}$	heat-transfer rate per unit area
Q	heat load per unit area
$\bar{t}$	smeared skin thickness
T	temperature
W	weight
x,y,z	model coordinates; full-scale orbiter stations

α	angle of attack
e	emissivity

Subscripts

aw	adiabatic wall
L	length
l	local
w	wall

APPARATUS AND TESTS

Facility

The experimental heat-transfer results presented herein were obtained in the Langley Continuous Flow Hypersonic Tunnel. This facility, which has a 78.75-cm (31-inch) square test section, operates at a nominal free-stream Mach number of 10.3 over a range of Reynolds number per meter of 1.5×10^6 to 8.2×10^6 (0.5×10^6 to 2.5×10^6 per foot) using air as the test gas. The facility may be operated in either a blowdown or continuous, closed-circuit mode. To prevent liquefaction, the air is heated to a temperature of 970 K (1750° R) by means of an electric-resistance tube heater. The tunnel throat, nozzle, and diffuser sections are all water-cooled.

For these tests, the model was mounted on the facility model-injection mechanism, which is adjacent to the test section. The device allows the model to be isolated from the hypersonic airstream for model cooling and configuration changes while the tunnel is operating. The mechanism also provides rapid injection of the model into the airstream to obtain transient heating on the relatively cool model.

Models

The models used in the heat-transfer tests were the 140 A/B orbiter-baseline configuration shown in figure 1(a) and the orbiter with the S-2 fillet and C-4 canard shown in figures 1(b) and 1(c). The two modifications were designed to minimize the hardware modification and scar weight which would be imposed on the shuttle orbiter. The S-2 fillet was designed to replace the planned baseline fillet. Most of the planform area added is distributed forward with one portion extending to station 300 on the forebody. The C-4 canard has the same attachment footprint as the baseline fillet and the trailing edge of the canard is designed to fair in with the baseline fillet at station 807. The entire canard attaches to the orbiter midfuselage section except for a small leading-edge fairing on the forebody. Both the S-2 fillet and C-4 canard were carefully faired into the lower surface of the orbiter with flat or convex surfaces. Concave surfaces were avoided because of possible adverse affect on boundary-layer transition. The weight penalty of the fillet is approximately half that for the C-4 canard, but the fillet installation affects a much larger portion of the body.

Models of the three configurations were cast in stycast 2762; the molds were made using the 0.01-scale force models with the elevons, body flap, and speed brakes set at zero deflection. Both the wing and canard surfaces were thickened on the upper surface toward the trailing edge in order to provide a sufficient thickness of the material for use of the phase-change testing techniques. Photographs of the three models are shown in figure 2.

To insure accurate knowledge of the thermal properties of each model, a test specimen was poured from the same mixed batch of stycast, as each model was cast and the samples went through the same cure cycle as the models. Thermal properties--conductivity, specific heat, and density--were measured on each of these samples for use in the data reduction.

Methods

The heat-transfer data were obtained by using the phase-change paint technique (ref. 5) and the melt line was recorded on a double frame 35-mm motion picture film, at the rate of 10 frames per second. Before applying the coating of the phase-change material the model temperature was allowed to come to room temperature. Initial temperature of the model was measured with a thermocouple, which was cast in the model, about 1 cm (0.4 inch) from the surface. A number of phase-change paints which had different melt temperatures were used. The selection of the melt temperature of the paint was usually a compromise between the need to obtain melting, before the high-temperature stream flow damaged the model or built up excessively large lateral conduction in the model and having a long enough time to melt so that the time period could be accurately measured. The lowest melt temperature of the paints used was 316 K (109^{o}F), in which case the paint melted over most of the sides of the model but produced little or no melting over upper surfaces of the fuselage and wings in the safe time period.

Oil-flow studies were conducted to examine the surface flow, relative shear, and separation boundaries on the upper surface of the body and wings. The same black stycast heat-transfer models were used in the oil-flow tests. The models were coated with a thin layer of silicon oil mixed with a white titanium oxide pigment prior to testing. The oil-flow patterns persisted at the end of the test allowing the models to be removed and photographed.

Data Reduction

The heat-transfer data were reduced to heat-transfer coefficients using the methods of reference 5. For the lower surface, a laminar recovery factor of 0.86, based on local conditions on a wedge at the angle of attack of the orbiter was used. Since the recovery factor is not known for the upper surface and side flows, a recovery factor of 1.0 was assumed. The local heat-transfer coefficient was normalized by the calculated stagnation heat-transfer coefficient (method of Fay and Riddell, ref. 6) on a sphere having a 0.305-m (1.0-foot) radius, scaled by the same factor as the model and at the tunnel test conditions.

RESULTS AND DISCUSSION

Flow-Field Characteristics

Surface oil-flow studies were conducted on the three configurations at an angle of attack of 30^{o} and a Reynolds number of 10^{6} based on model length. On the lower surface, the addition of the S-2 fillet and C-4 canard configurations to the baseline configuration caused no important change in the streamline patterns as indicated by the oil streaks. On the orbiter sides and upper wing/fuselage areas, the oil flow indicated the presence of several vortices and relatively larger areas of separated flow with low shear. Photographs of the oil-flow patterns on the side and upper surfaces of the three configurations are shown in figure 3. Oil streaks occur in regions of high shear, indicating surface flow directions. The oil usually accumulates on the surface where the flow

separates. In separated flow regions or regions of low shear, the oil may not move. but one can frequently see the brush marks of the original oil coating.

A vortex-interference pattern is seen on the fuselage side on each of the configurations, but its origin is located farther forward on the S-2 fillet model as a result of the larger span of the wing and the farther-forward location of the wing junction with the body. Because of the intensity of this vortex which appears to originate at the juncture of the wing leading edge with the body, additional fairings of the juncture were made and tested. These fairings of the juncture, some of which were quite extensive, did not significantly affect the flow pattern observed in the oil flow. It was concluded that the flow pattern on the side of the fuselage is a result of the reattaching shear layer, which has its origin on the leading edge of the wing. This flow on the fuselage side usually separates at about the body shoulder; however, where the shear layer attachment appeared to be most intense, the flow remains attached for a small distance over the top of the body. The flow interpretations made from the oil-flow studies is in agreement with the flow model deduced from the heat-transfer measurements.

At these test conditions, strong vortices were not present in the customary location on the top of the fuselage. Several very weak vortices, a primary vortex on the centerline and a secondary vortex between the centerline and the shoulder were faintly visible in the oil flow, but are not apparent in the photographs.

The flow is attached over a significant portion of the upper surface of the wing and separates at about the same chordwise location for all three configurations. Near the body where the wing leading edge is highly swept, the flow separates at about the leading edge. At the angles of attack of the present tests, the larger span of the S-2 fillet configuration effectively shields the Orbital Maneuver Subsystem (OMS) pod and the vertical tail from the oncoming flow.

Heat Transfer

Lower surface.- In order to enhance the confidence in the present test series, which used the phase-change paint method of measuring heat transfer, the lower-surface centerline heat-transfer coefficients (ratioed to a 0.305-m (1-foot) radius sphere heat-transfer coefficient) measured in the present tests are compared with results of baseline orbiter configuration tests in the Ames Research Center 3.5-Foot Wind Tunnel, which used the thin-skin thermocouple technique. The comparison is shown in figure 4. The Ames Research Center results are at a Reynolds number between the high and low Reynolds number data of the present tests. The lower-surface flow in all cases appears to be laminar, and the level and distribution of heat transfer, for both the high and low Reynolds number results of the present phase-change tests, are in good agreement with those obtained using the thin-skin thermocouple technique.

Lower-surface heating contours for the three tests conditions, $\alpha = 30^{o}$ at $Re_L = 10^6$ and 2×10^6 and $\alpha = 40^{o}$ at $Re_L = 10^6$, are shown in figure 5 for the three configurations. General features of the heating distributions are

similar for all three configurations. For all three configurations, the heating rate decreases in the stream direction all the way to the trailing edge, indicating the flow is laminar. Increased heating is noted on the leading edge where the bow-shock intersection is expected. The vortex which usually emanates from this intersection and crosses the wing tip, causing boundary-layer transition and high heating in the wing-tip region, is not present. It is also notable that there is no shock impingement on the leading edge of the canard on that configuration. In order to compare directly the heating to the three configurations, centerline-heating distributions and spanwise heating distributions at $X/L = 0.5$ and 0.8 were plotted and are shown in figures 6 and 7. The general character of heating distribution is similar for all three configurations. The heating levels shown in these figures do not indicate a substantial difference between the configurations, nor can any one of the configurations be identified as having less heating at all three test conditions than any of the others. Thus, it is concluded that no significant adverse effects have been produced on the baseline lower-surface heating by the addition of either of the configuration modifications.

Fuselage side.- A shear-layer impingement, heat-transfer pattern is present on the sides of the three configurations and the shape changes of the retrofit packages produce large differences in the heat transfer. Side heat-transfer contours for the configuration at the three test conditions are shown in figure 8. Although the heat-transfer contours give the appearance of resulting from a vortex emanating from the juncture of the wing/wing-fillet with the body, the heating is believed to be the result of the separated shear layer from the wing or fillet leading edge reattaching on the side of the fuselage. The S-2 fillet configuration has a considerably smaller interference heating pattern which is located farther forward on the side. Due to the larger local span of the fillet than the baseline, the shear layer from the leading-edge separation passes off the fuselage side farther forward than on the other two configurations. The increased span of the S-2 fillet configuration is effective in shielding the OMS pod and the vertical tail from the separated shear-layer flow at $\alpha = 30^{o}$; at the higher angle of attack the shear layer does not impinge on the vertical tail or the OMS pod to as great a degree as at the lower angle of attack. The changes in heat transfer due to the retrofits appear to be relatively large for the sides of the fuselage and this will be evaluated in terms of increased TPS weight in a later section.

Boundary-layer transition.- As already stated, no evidence of boundary-layer transition was seen in the heat-transfer distributions for any of the configurations of the present tests. Early boundary-layer transition is of considerable concern since previous tests at a Mach number of 8 (unpublished) of a shuttle orbiter with adjustable trimmers (which are similar in planform and location to the C-4 canard) showed a large affect on the boundary-layer transition location. Criterion for the onset of boundary-layer transition has been generated from hypersonic wind-tunnel tests on orbiter configurations and for much of the design period this criterion has been $Re_{\theta}/M_{l} = 225$. Values of this parameter on the centerline at the trailing edge of the model for the present tests conditions are:

α	Re_L	(Re_θ/M_1)
30°	1×10^6	167
30°	2×10^6	246
40°	1×10^6	219

The highest of these values is only approximately equal to the developed transition onset criterion; however, had there been a significant adverse effect on boundary-layer transition as a result of either the fillet or canard retrofit modifications, boundary-layer transition should have been observed in the heat-transfer distributions. One important difference between the configurations of the present tests and those where the adverse transition effects were observed is that the canards and fillets were smoothly faired into the lower surface without any concave curvature. Such smooth fairings were not achieved in the tests of the adjustable trimmers. For the present study, it is concluded that the addition of the retrofits to the baseline configuration would not adversely affect boundary-layer transition.

Impact of retrofits on TPS weight.- The sides of the fuselage are the areas of the configurations where the reentry heating rates are most strongly affected by the addition of the retrofits, and for these areas the change in the weight of the TPS is calculated. Reference heating rates used in making estimates of the orbiter side TPS weight are shown in figure 9. Trajectory 14414.1 is being used to design the TPS on the Space Shuttle Orbiter. The TPS thickness is determined by the total heat load, Q, which is considerably less for the higher angle-of-attack entry. Radiation equilibrium surface temperature is shown as a function of heating-rate ratio in figure 10. Heating rates on the sides of the orbiter configurations will produce surface temperatures well below the maximum temperature limit of the RSI.

TPS weights were calculated for LI-900 Reusable Surface Insulation (RSI) material which has a density of 146 kg/m^3 (9 lbs/ft^3). The thickness of material required is shown in figure 11 as a function of the heat load and backface heat-sink capacity (smeared aluminum skin thickness $\bar{t}$). For these calculations the skin thickness was assumed to be 0.25 cm (0.1 inch). In figure 12, the unit weights of LI-900 RSI on one side of the configurations are shown as a function of the areas covered. The area under each curve is an indication of the side TPS weight. Interference heating on the orbiter side is located in quite different areas for the various configurations. The unit weights labeled "baseline + retrofit configuration" are for side-heating distributions, which are the maximum heating of the two configurations combined. The use of the S-2 fillet or C-4 canard retrofits would require this weight of TPS on the side. Note that at $\alpha = 40°$, figure 12(c), the areas under the unit-weight curves are smaller; this reflects the reduced size of the interference-heating region and the lower total heat load of the higher angle-of-attack entry.

Orbiter side TPS weights (the vertical tail and OMS pod areas are not included) for an LI-900 RSI system are shown in table I for the baseline, S-2 fillet and C-4 canard configuration based on data from the three test conditions

(weights are for two sides of the configurations). These weights are not the total side TPS weight, but reflect the weight of TPS required to protect the area of high interference heating. Heating to other areas would be covered with minimum gage material and presumably equal for all the configurations.

Delta side TPS weights for the S-2 fillet and C-4 canard configurations are given in table II. The S-2 fillet configuration had a beneficial effect on the TPS weight at several test conditions. The C-4 canard required additional material at all test conditions. The weights shown in table II are for TPS designed specifically for the test heating distributions; however, the expected use of the S-2 fillet and C-4 canard is as retrofits, and the side TPS of the orbiter is not apt to be changed when the retrofit is added. Thus, the side TPS would be designed for the highest heating which results from the combined baseline and proposed retrofit configuration heating distributions. Resulting delta TPS weights for this situation are shown in table III, and these weights are the scar weights or weights of TPS material, which must be added to the two sides of the baseline vehicle to allow reentry in the baseline configuration with the proposed retrofit configuration. These scar weights are small in comparison to the total weights for the retrofit packages which are approximately 500 and 750 kg (1100 and 1650 lbs) for fillet and canard retrofit configurations.

SUMMARY OF RESULTS

Heat-transfer studies were conducted at Mach 10.3, on Space Shuttle Orbiter models with the S-2 fillet and C-4 canard retrofit moldlines, which were generated in aerodynamic and system-design studies to increase the allowable c.g. range of the orbiter. From the heat-transfer results and analytical studies of the heating effects on the TPS, the following were concluded.

1. No boundary-layer transition was observed at $M = 10.3$ on any of the configurations at Re_θ/M_1 approximately equal to the orbiter transition criterion. The well-faired retrofit configurations did not adversely affect boundary-layer transition as in previous tests.

2. The lower-surface heating was not significantly altered by the proposed changes to the configurations.

3. The area affected by the shear-layer impingement on fuselage side of the orbiter was, in general, larger for the baseline and C-4 canard configurations than the S-2 fillet configuration.

4. Scar weight of the orbiter-side TPS, due to allowances for retrofit of the S-2 fillet and C-4 canard, are small (less than about 90 kg (200 lbs)) in comparison to the total weight of the retrofit.

References

1. Phillips, Pelham W.: Space Shuttle Orbiter Trimmed Center-of-Gravity Extension Study, Volume II - Effects of Configuration Modifications on the Aerodynamic Characteristics of the 140 A/B Orbiter at Transonic Speeds. NASA TM X-72661, 1976.

2. Bernot, Peter T.: Space Shuttle Orbiter Trimmed Center-of-Gravity Extension Study, Volume I - Effects of Configuration Modifications on the Aerodynamic Characteristics of the 140 A/B Orbiter at M = 10.3. NASA TM X-72661, 1975.

3. Scallion, William I.; and Stone, David R.: Space Shuttle Orbiter Trimmed Center-of-Gravity Extension Study, Volume IV - Effects of Configuration Modifications on the Aerodynamic Characteristics of the 139B Orbiter at Mach 20.3. NASA TM X-72661, 1978.

4. MacConochie, Ian O.: Space Shuttle Orbiter Trimmed Center-of-Gravity Extension Study, Volume VI - System Design Studies. NASA TM X-72661, 1978.

5. Jones, Robert A.; and Hunt, James L.: Use of Fusible Temperature Indicators for Obtaining Quantitative Heat-Transfer Data. NASA TR R-230, 1966.

6. Fay, J. A.; and Riddell, F. R.: Theory of Stagnation Paint Heat Transfer in Dissociated Air. J. Aeronaut. Sci., vol. 25, no. 2, February 1958, pp. 73-85, 12.

TABLE I - ORBITER SIDE TPS WEIGHTS

CONFIGURATION	TPS WT, kg (LB)		
	$\alpha = 30^0$ $Re_L = 1 \times 10^6$	$\alpha = 30^0$ $Re_L = 2 \times 10^6$	$\alpha = 40^0$ $Re_L = 1 \times 10^6$
BASELINE	188 (414)	184 (406)	156 (343)
S-2 FILLET	200 (440)	144 (318)	150 (330)
C-4 CANARD	196 (432)	218 (480)	219 (482)

TABLE II - ORBITER SIDE RELATIVE TPS WEIGHTS

CONFIGURATION	$(TPS\ WT)-(TPS\ WT)_{BASELINE}$, kg(LB)		
	$\alpha = 30^0$ $Re_L = 1 \times 10^6$	$\alpha = 30^0$ $Re_L = 2 \times 10^6$	$\alpha = 40^0$ $Re_L = 1 \times 10^6$
BASELINE	0	0	0
S-2 FILLET	12 (26)	-40 (-88)	-6 (-13)
C-4 CANARD	8 (18)	34 (74)	63 (139)

TABLE III - ORBITER SIDE TPS WEIGHTS
TO ACCOMMODATE MODIFICATIONS

CONFIGURATION	$(TPS\ WT)-(TPS\ WT)_{BASELINE}$, kg (LB)		
	$\alpha = 30^0$ $Re_L = 1 \times 10^6$	$\alpha = 30^0$ $Re_L = 2 \times 10^6$	$\alpha = 40^0$ $Re_L = 1 \times 10^6$
BASELINE	0	0	0
S-2 FILLET	84 (184)	23 (51)	4 (9)
C-4 CANARD	79 (176)	80 (176	64 (144)

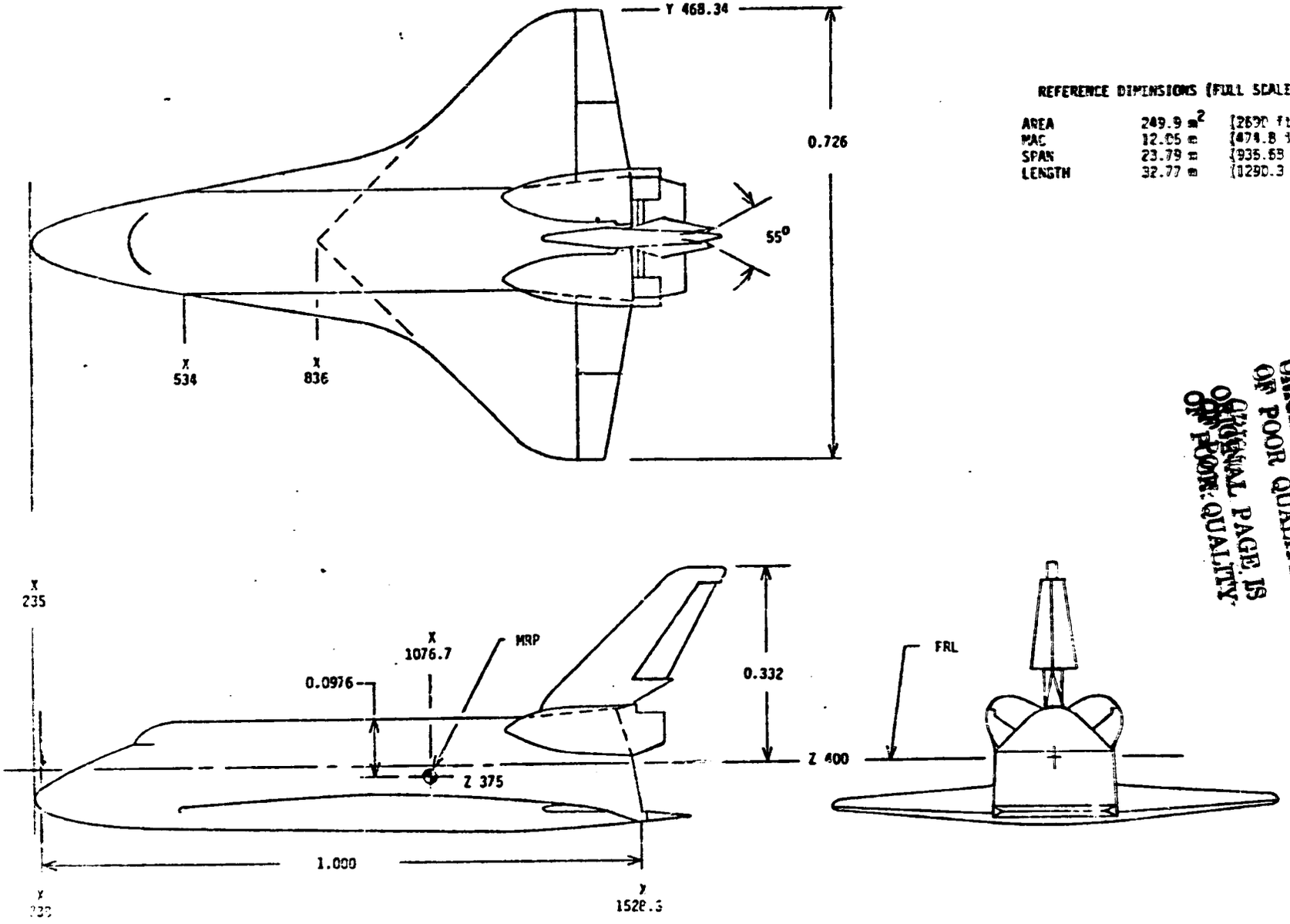

REFERENCE DIMENSIONS (FULL SCALE)

AREA	249.9 m^2	(2690 $ft.^2$)
MAC	12.05 m	(474.8 in.)
SPAN	23.79 m	(935.65 in.)
LENGTH	32.77 m	(1290.3 in.)

(a) 140 A/B orbiter baseline model

Figure 1.- Sketches of baseline orbiter and modifications. Locations x, y, and z indicate full-scale orbiter stations. Other geometric dimensions are normalized to reference body length.

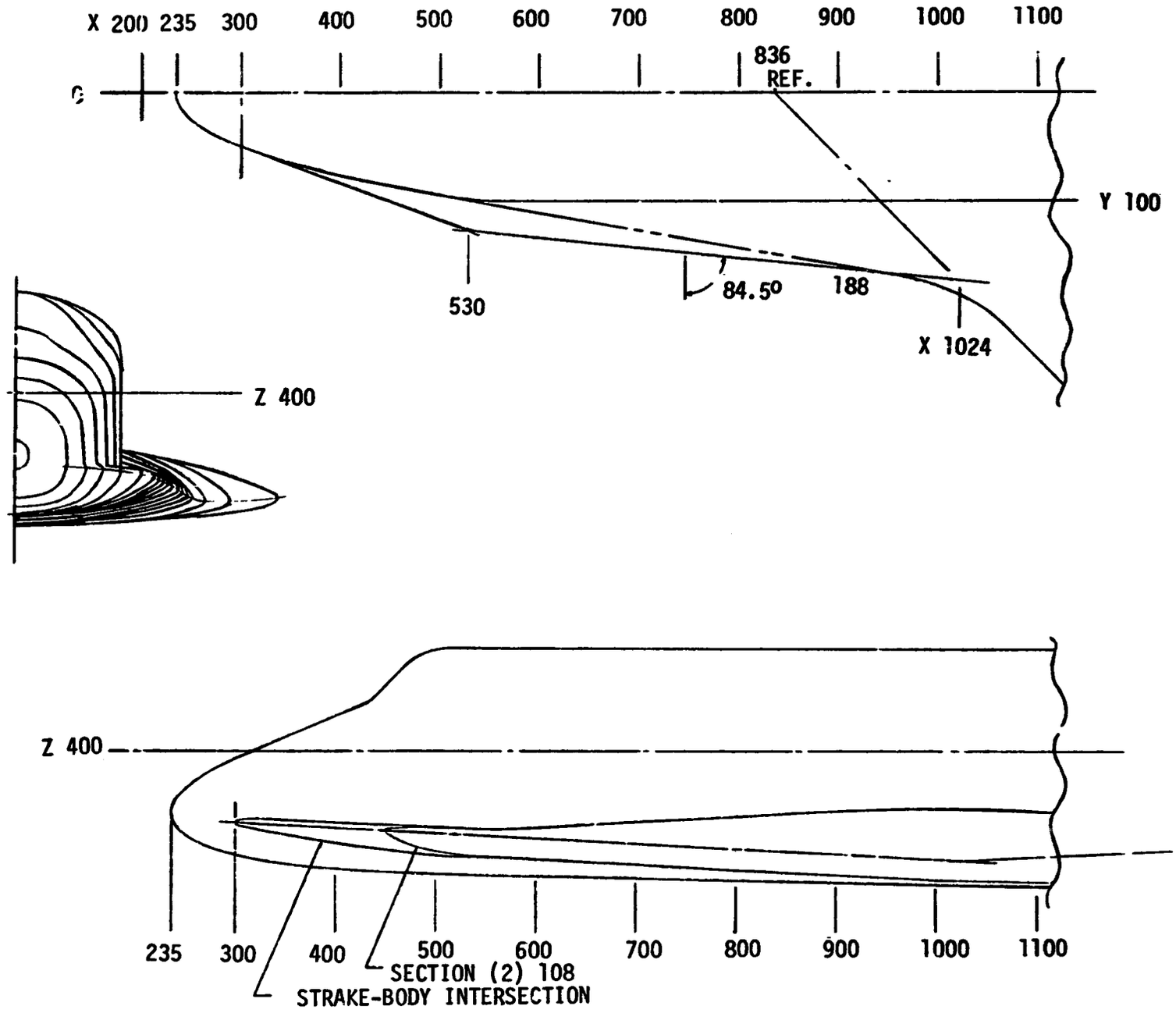

(b) S-2 fillet

Figure 1.- Continued

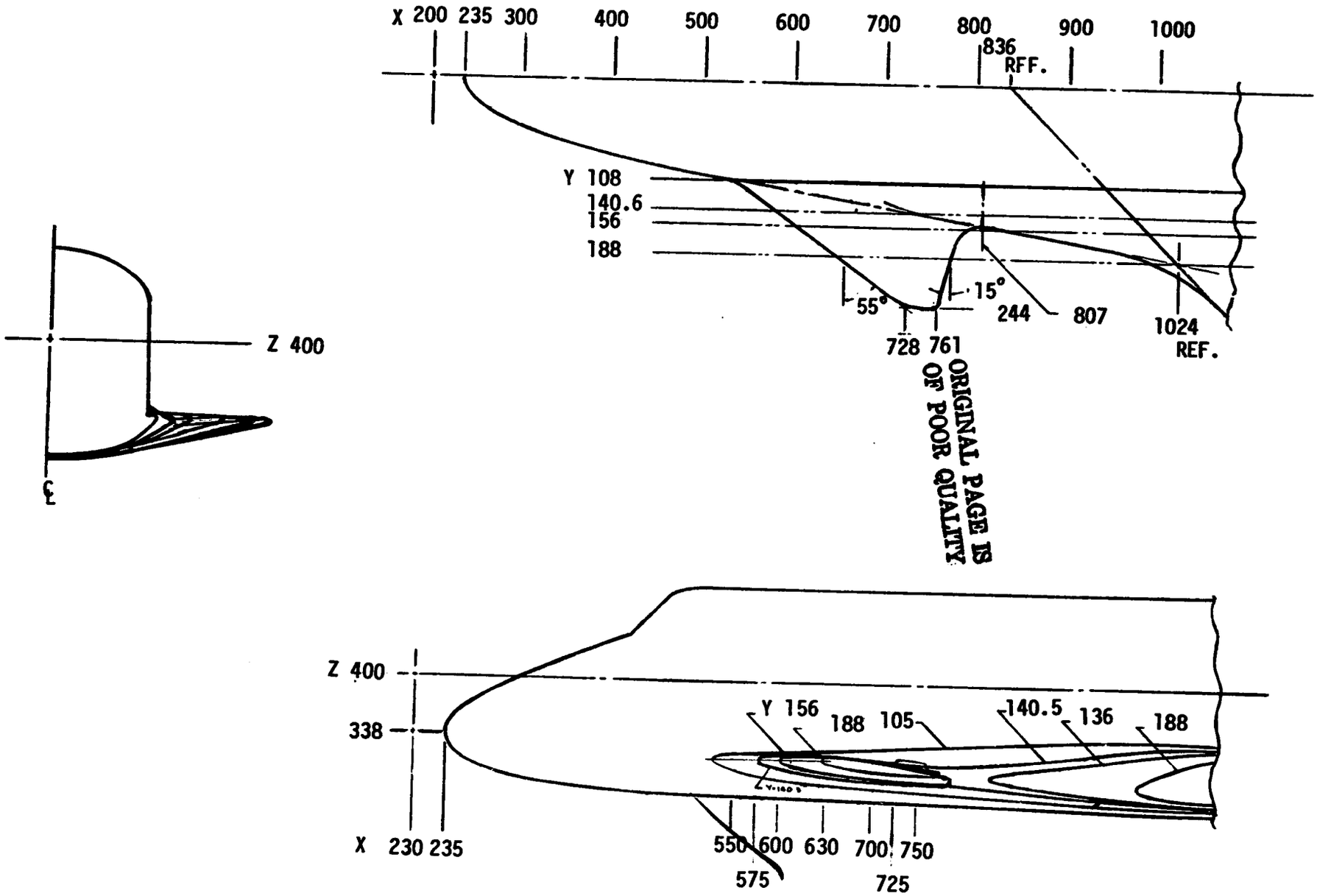

(c) C-4 canard

Figure 1.- Concluded

(a) 140 A/B orbiter baseline model

Figure 2.- Photographs of stycast models

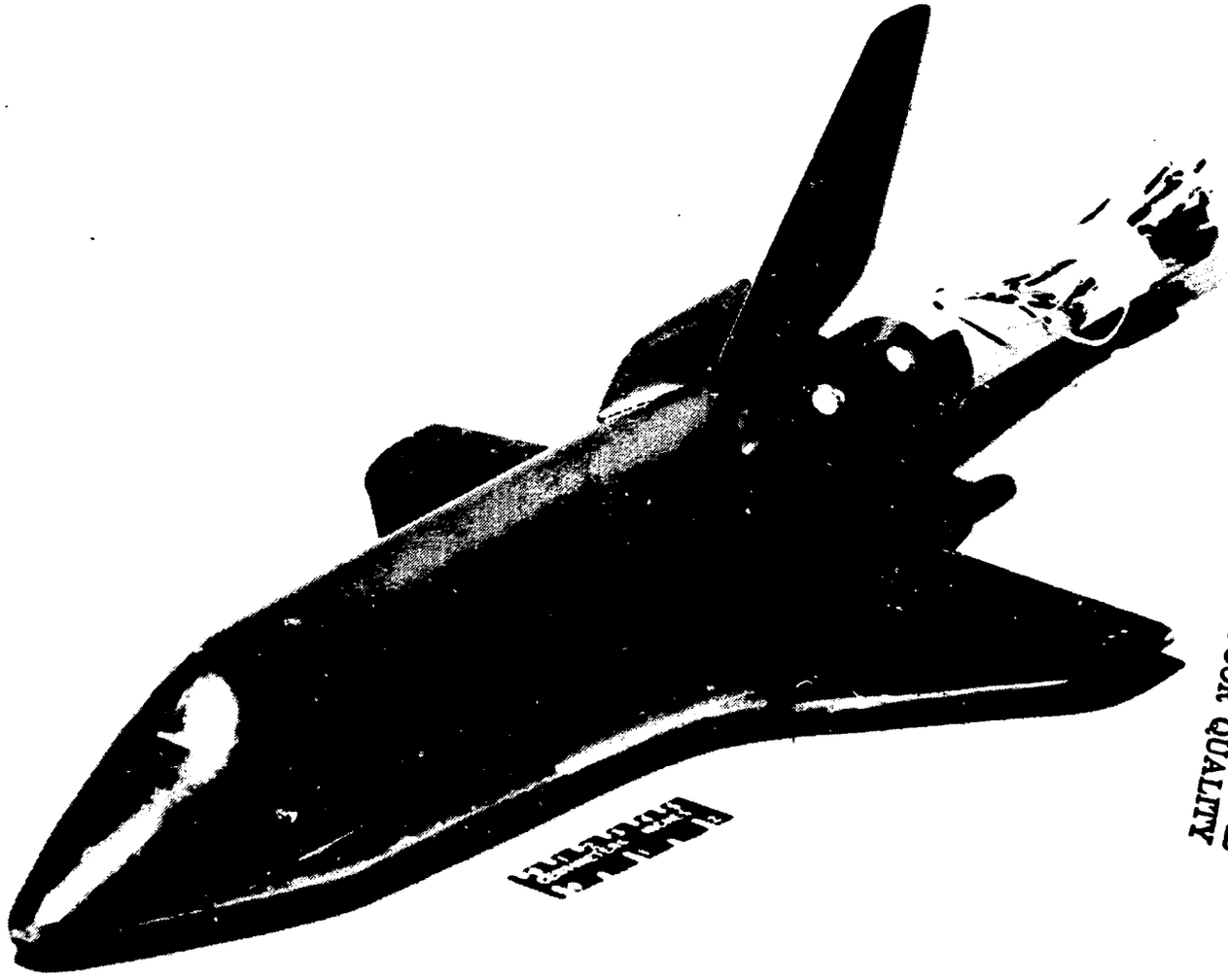

(b) S-2 fillet model

Figure 2.- Continued

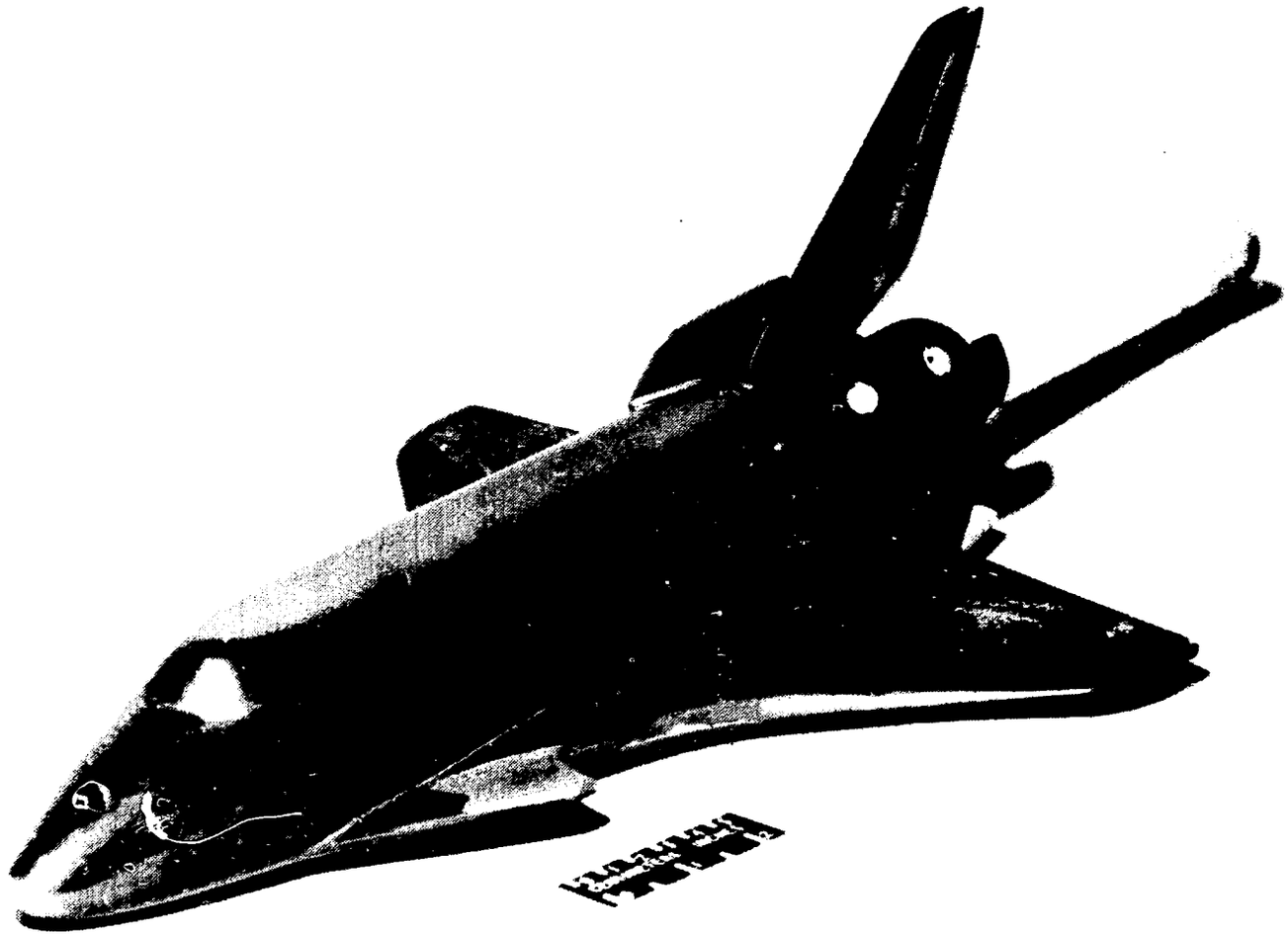

(c) C-4 canard model

Figure 2.- Concluded.

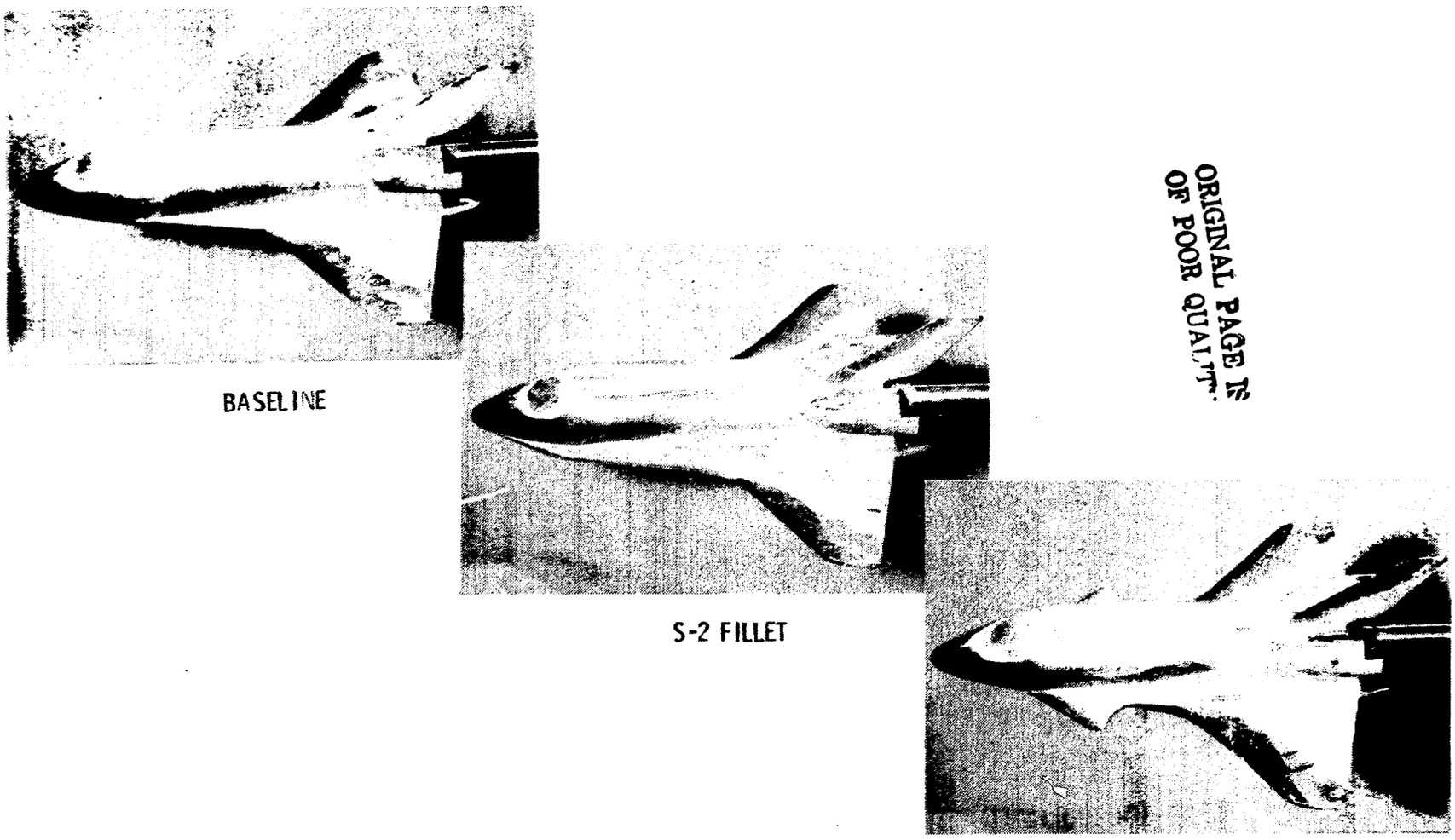

Figure 3. - Photographs of surface oil-flow patterns on baseline, S-2 fillet and C-4 canard shuttle orbiter models. $M = 10.3$, $\alpha = 30^{0}$, and $Re_{L} = 10^{6}$.

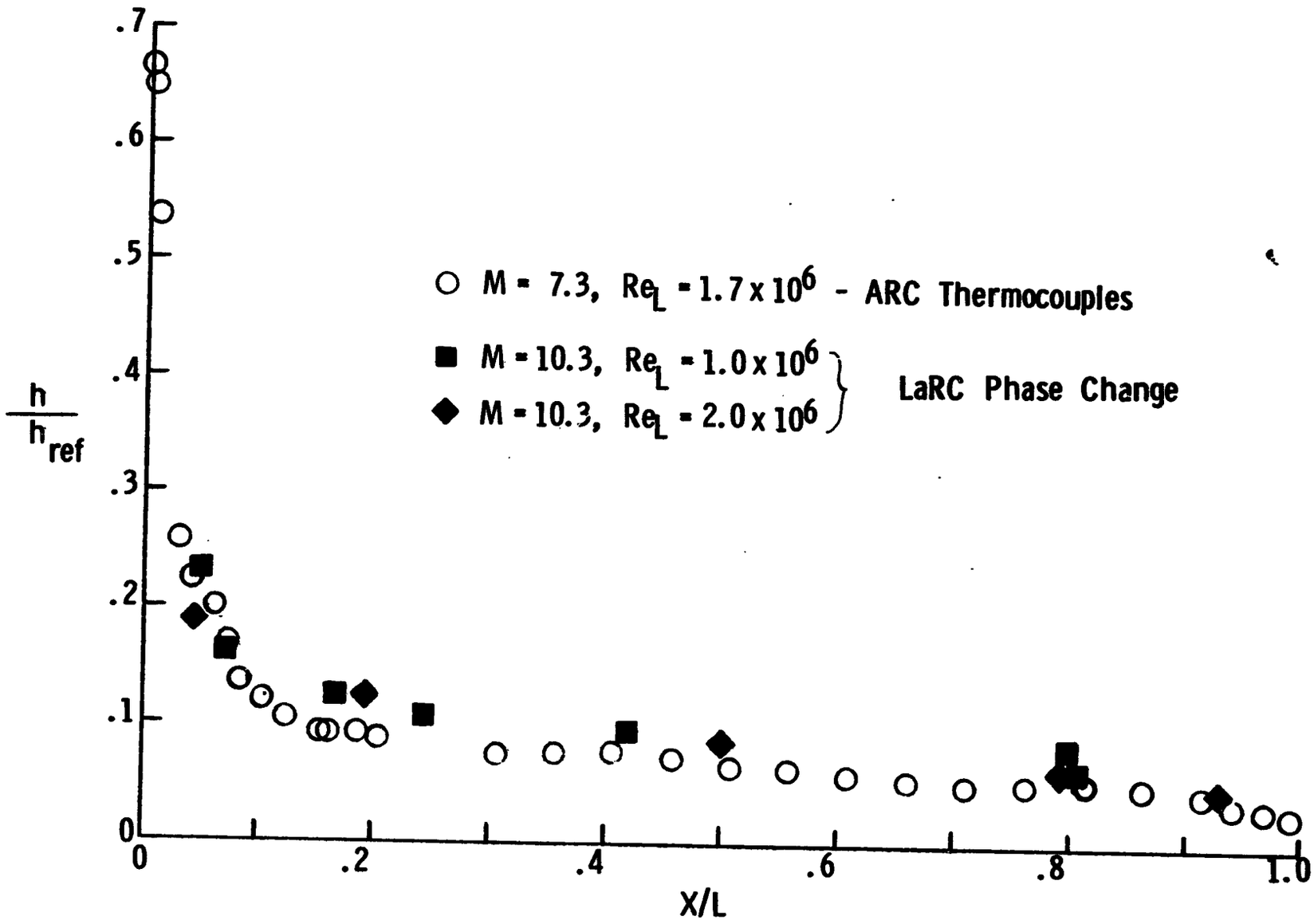

Figure 4.- Comparison of lower surface centerline heat-transfer distributions on 140 A/B shuttle orbiter. $\alpha = 30^{0}$.

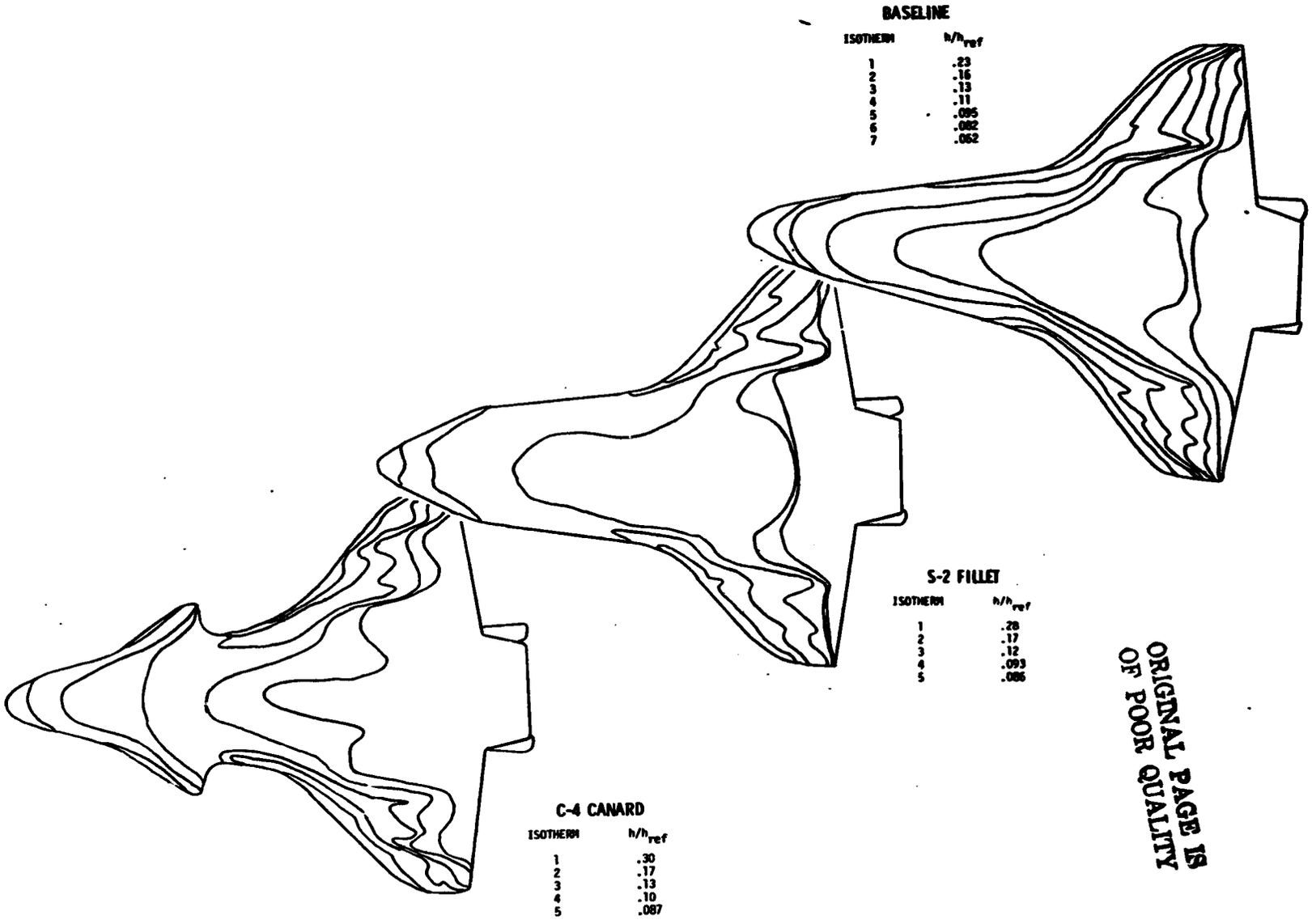

(a) $\alpha = 30^0$, $Re_L = 10^6$

Figure 5. - Lower surface heat transfer contours on baseline. S-2 fillet and C-4 canard shuttle orbiter models. M = 10.3.

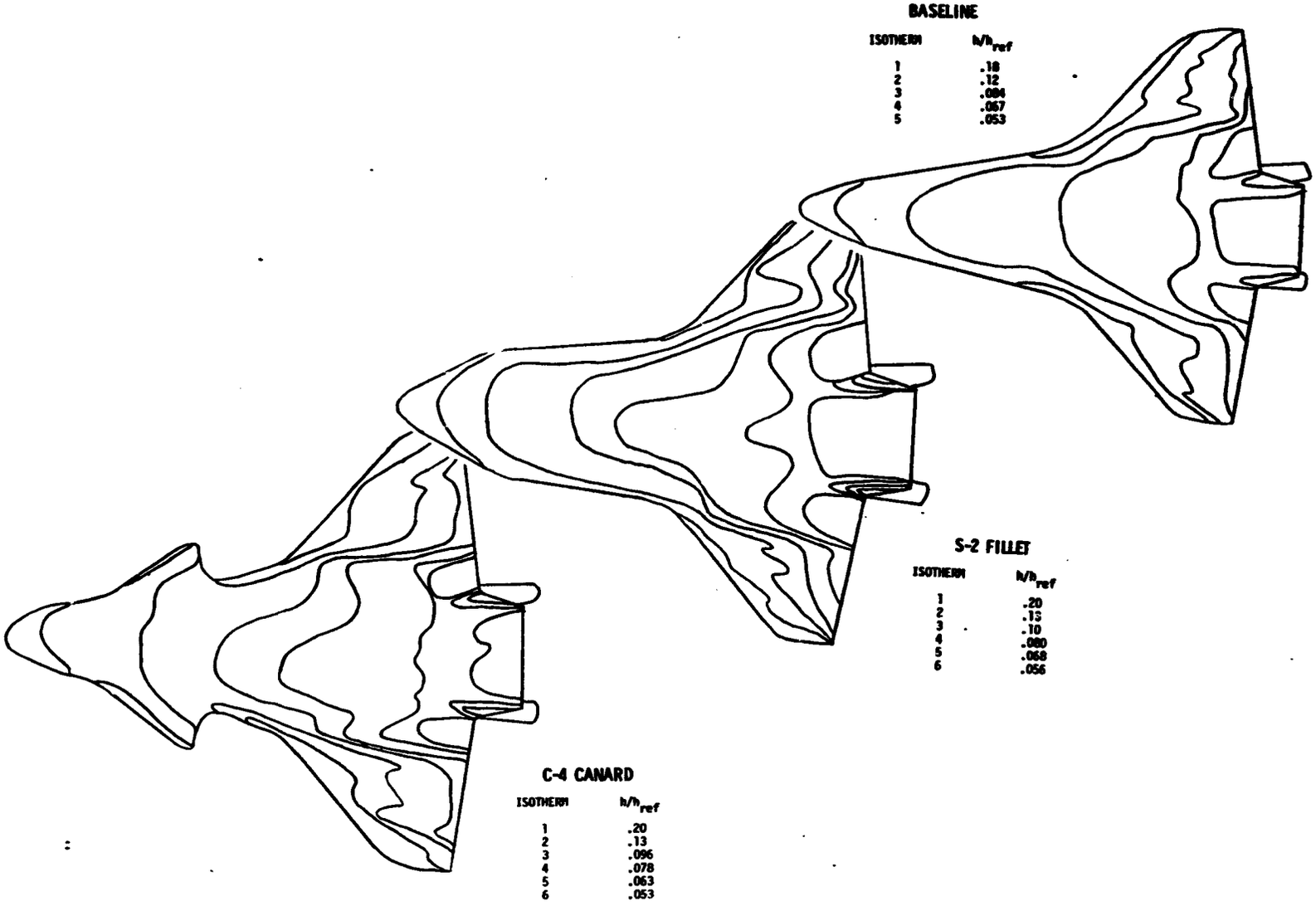

(b) $\alpha = 30^0$, $Re_L = 2 \times 10^6$

Figure 5. - Continued

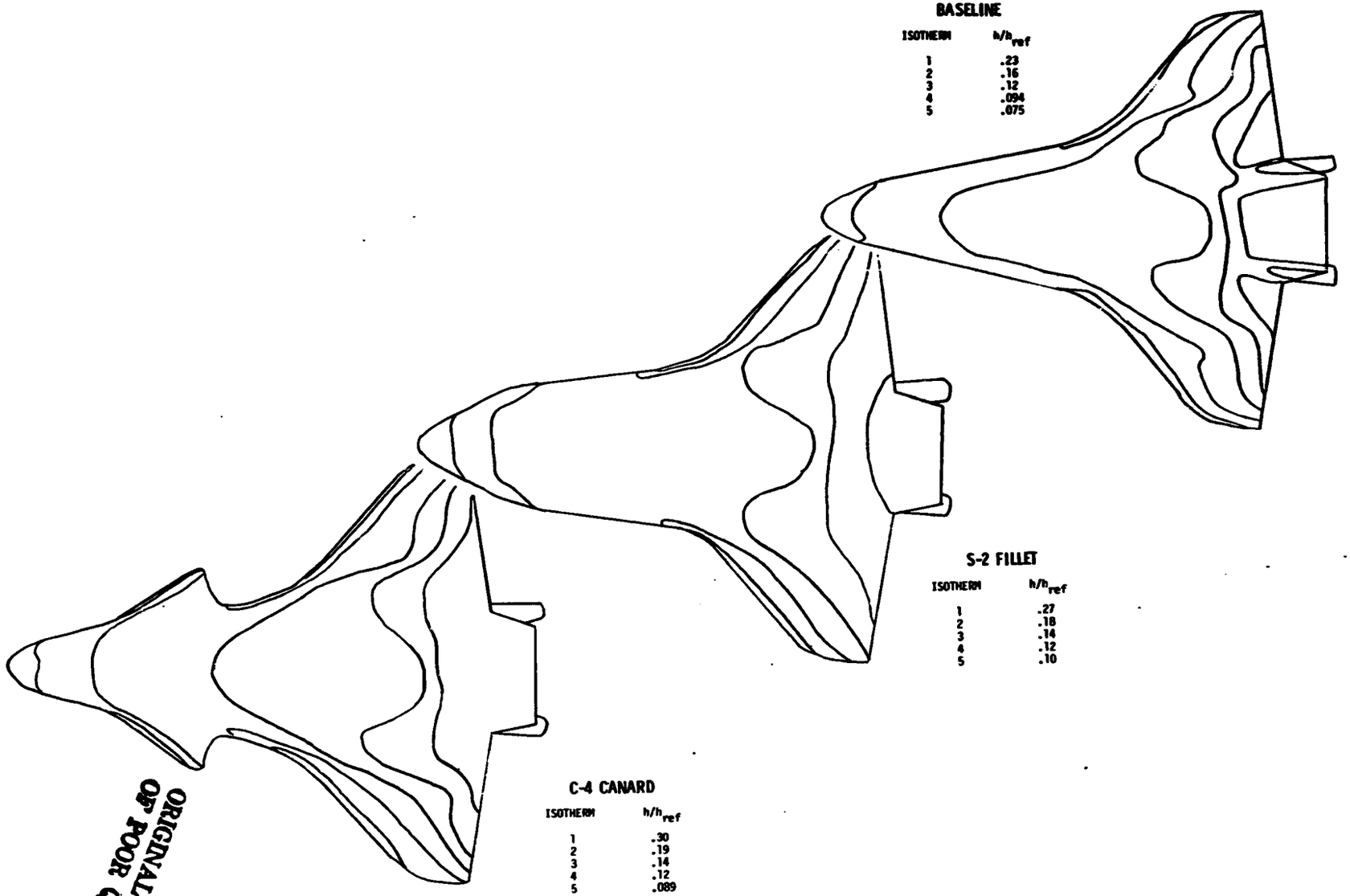

(c) $\alpha = 40^0$, $Re_L = 10^6$

Figure 5. - Concluded.

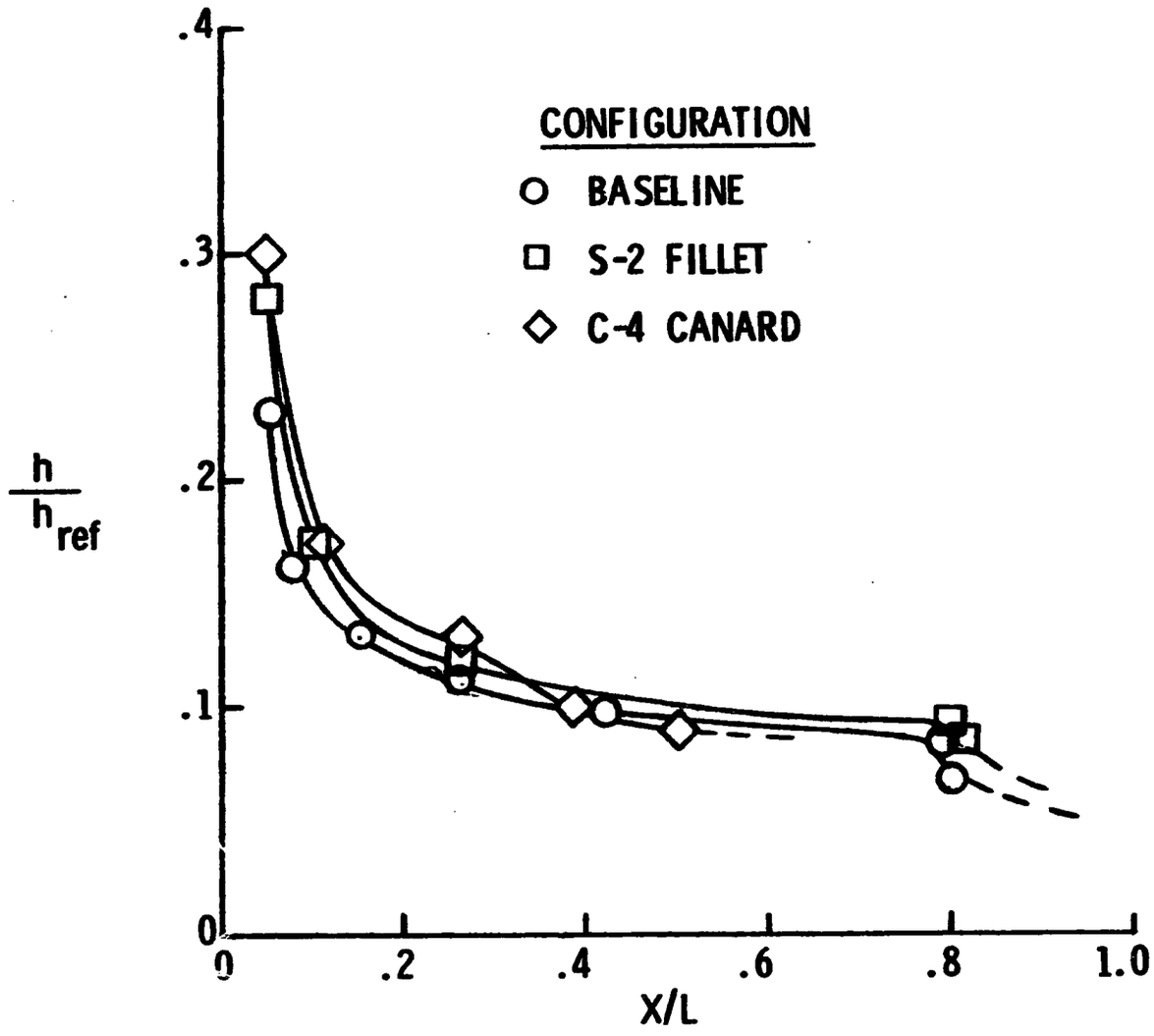

(a) $\alpha = 30^{o}$, $Re_L = 10^6$

Figure 6.- Comparison of heating to lower-surface centerline of baseline, S-2 fillet and C-4 canard shuttle orbiter models. $M_\infty = 10.3$

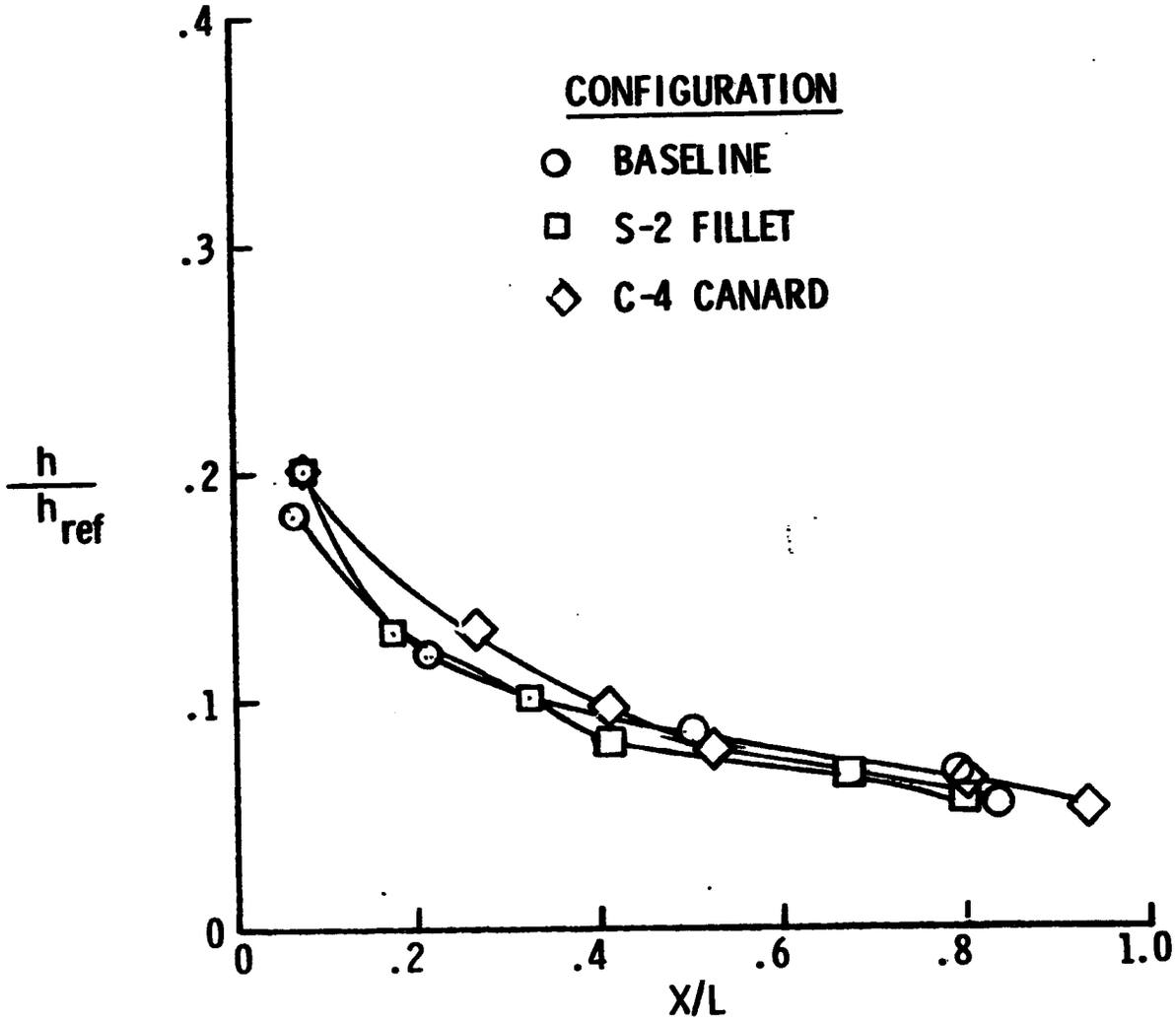

(b) $\alpha = 30^{o}$, $Re_L = 2 \times 10^6$

Figure 6.- Continued.

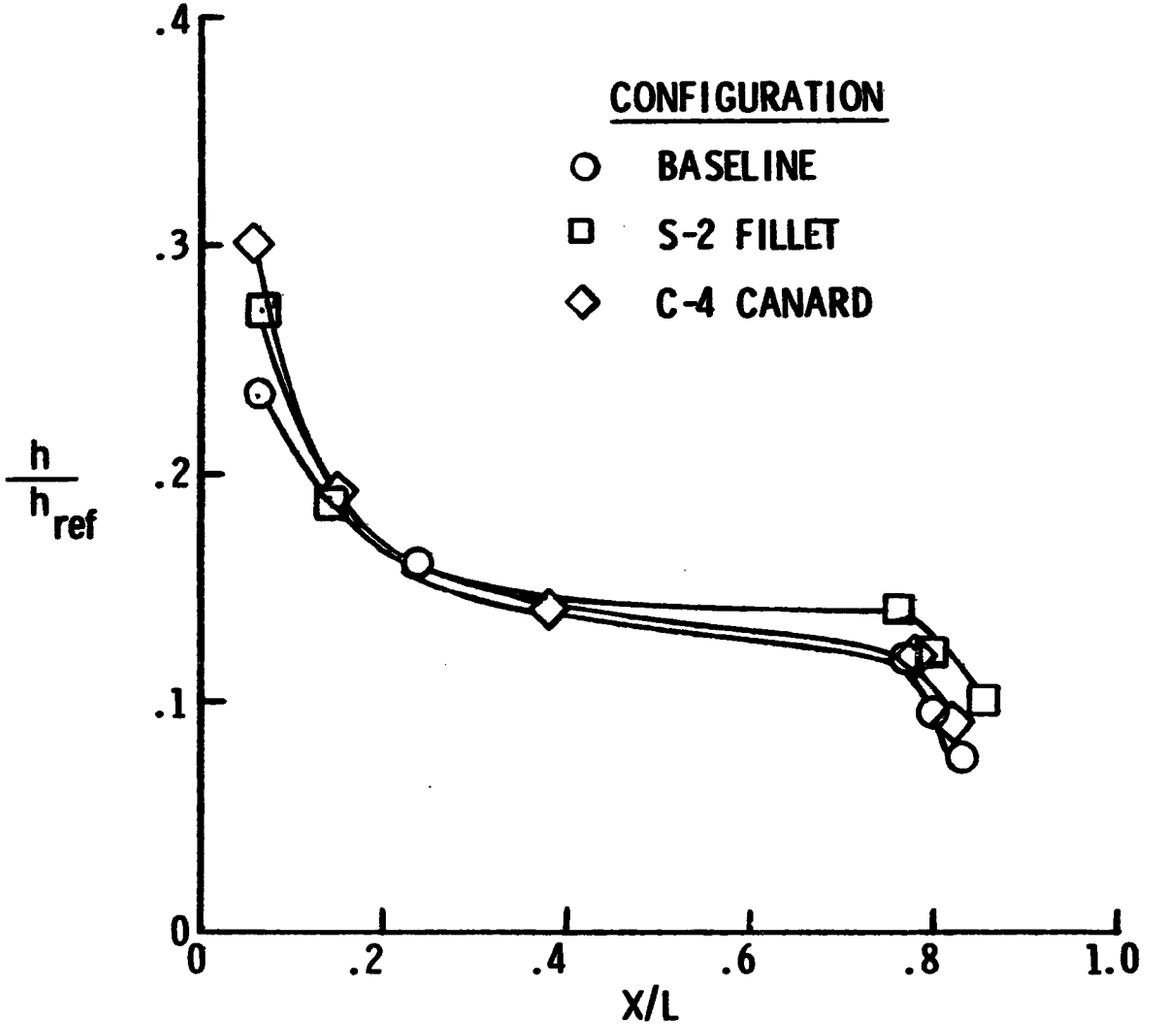

(c) $\alpha = 40^{o}$, $Re_L = 10^6$

Figure 6.- Concluded.

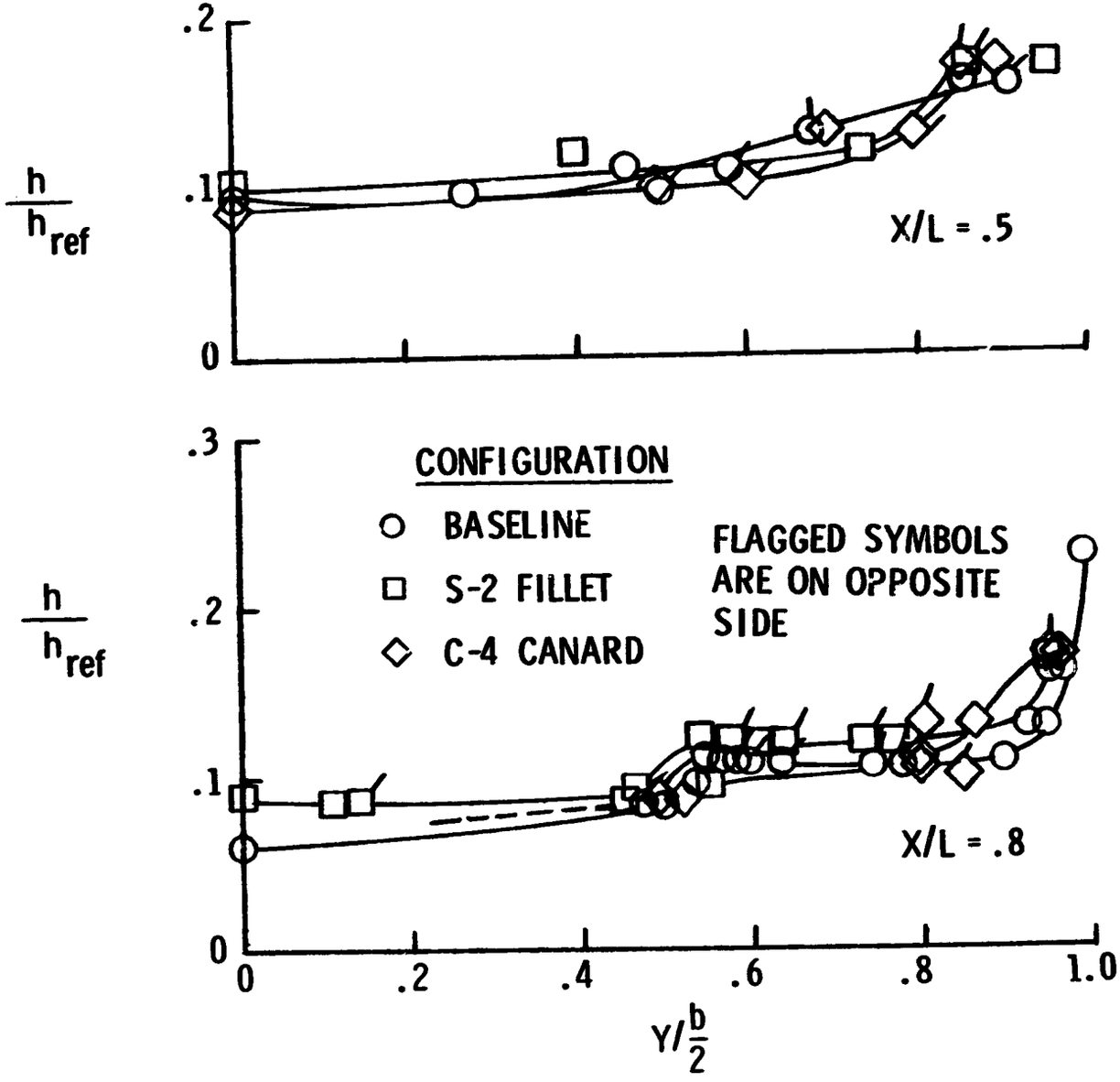

(a) $\alpha = 30^{o}$, $Re_L = 10^6$

Figure 7.- Comparison of lower surface spanwise heating distributions on baseline, S-2 fillet and C-4 canard shuttle orbiter models. $M_\infty = 10.3$.

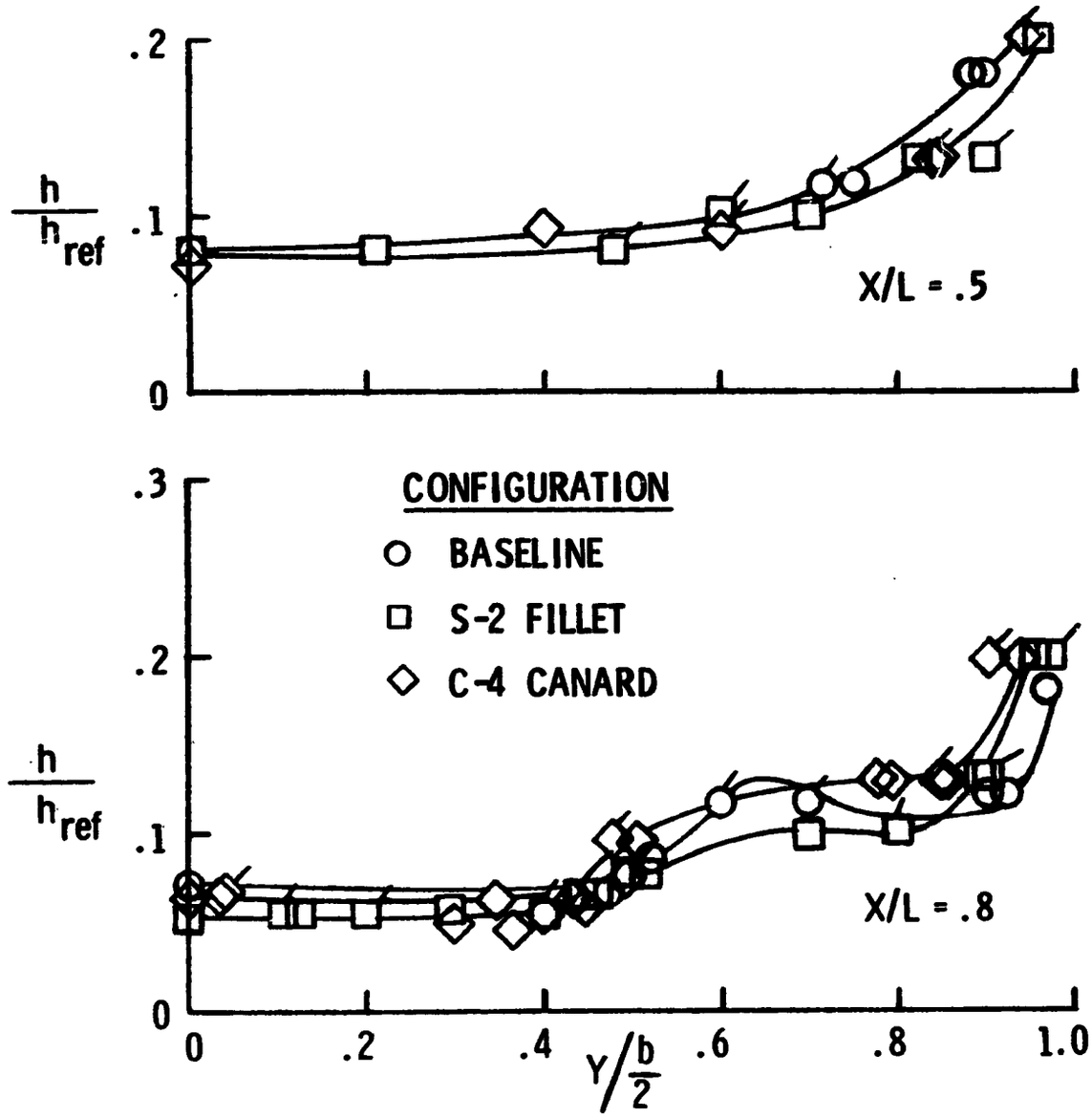

(b) $\alpha = 30^0$, $Re_L = 2 \times 10^6$

Figure 7.- Continued.

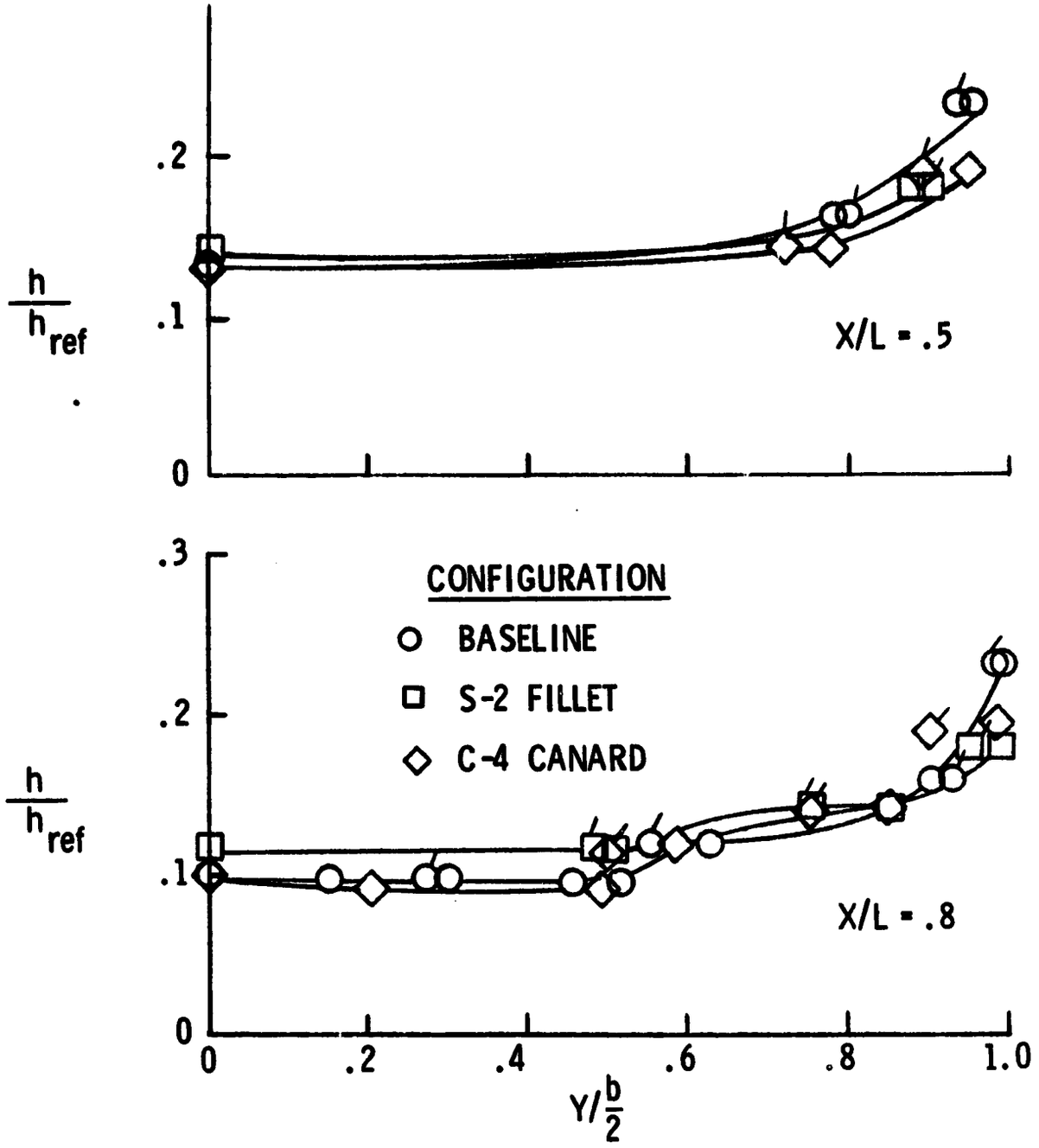

(c) $\alpha = 40^0$, $Re_L = 10^6$

Figure 7.- Concluded.

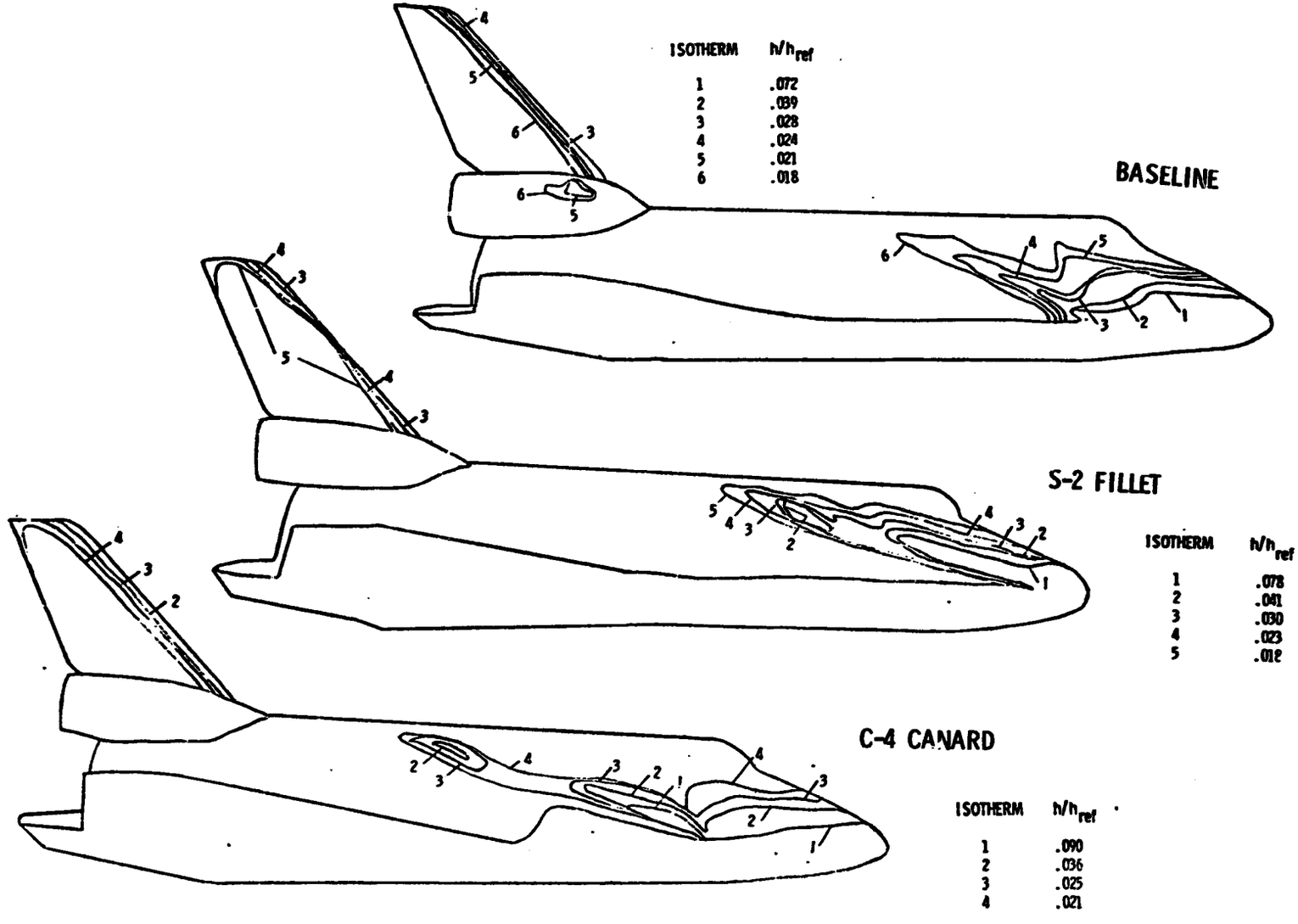

(a) $\alpha = 30^0$, $Re_L = 10^6$

Figure 8.- Heat-transfer contours on the side of baseline, S-2 fillet and C-4 canard shuttle orbiter models. $M_\infty = 10.3$.

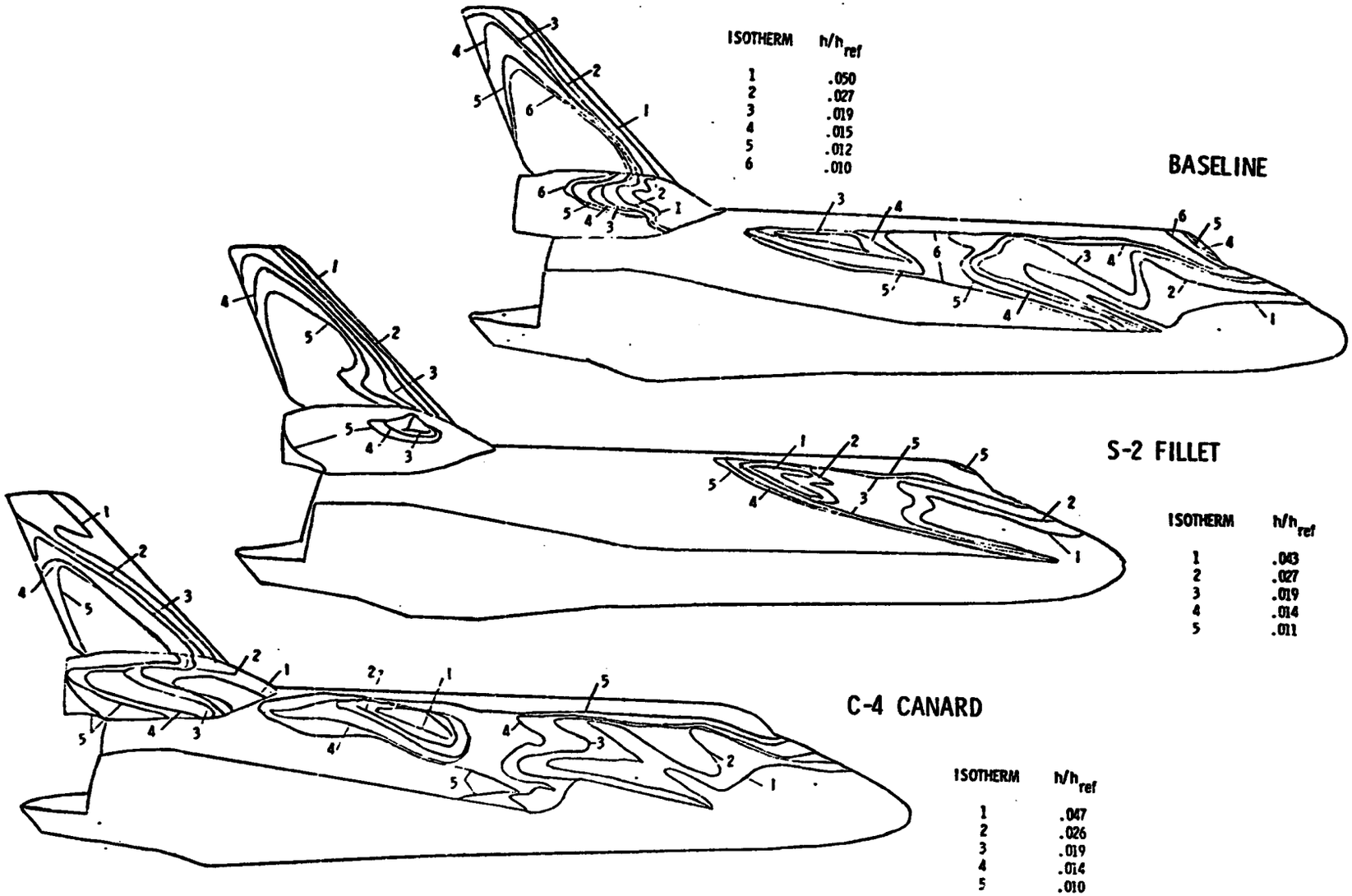

(b) $\alpha = 30^0$, $Re_L = 2 \times 10^6$

Figure 8. - Continued.

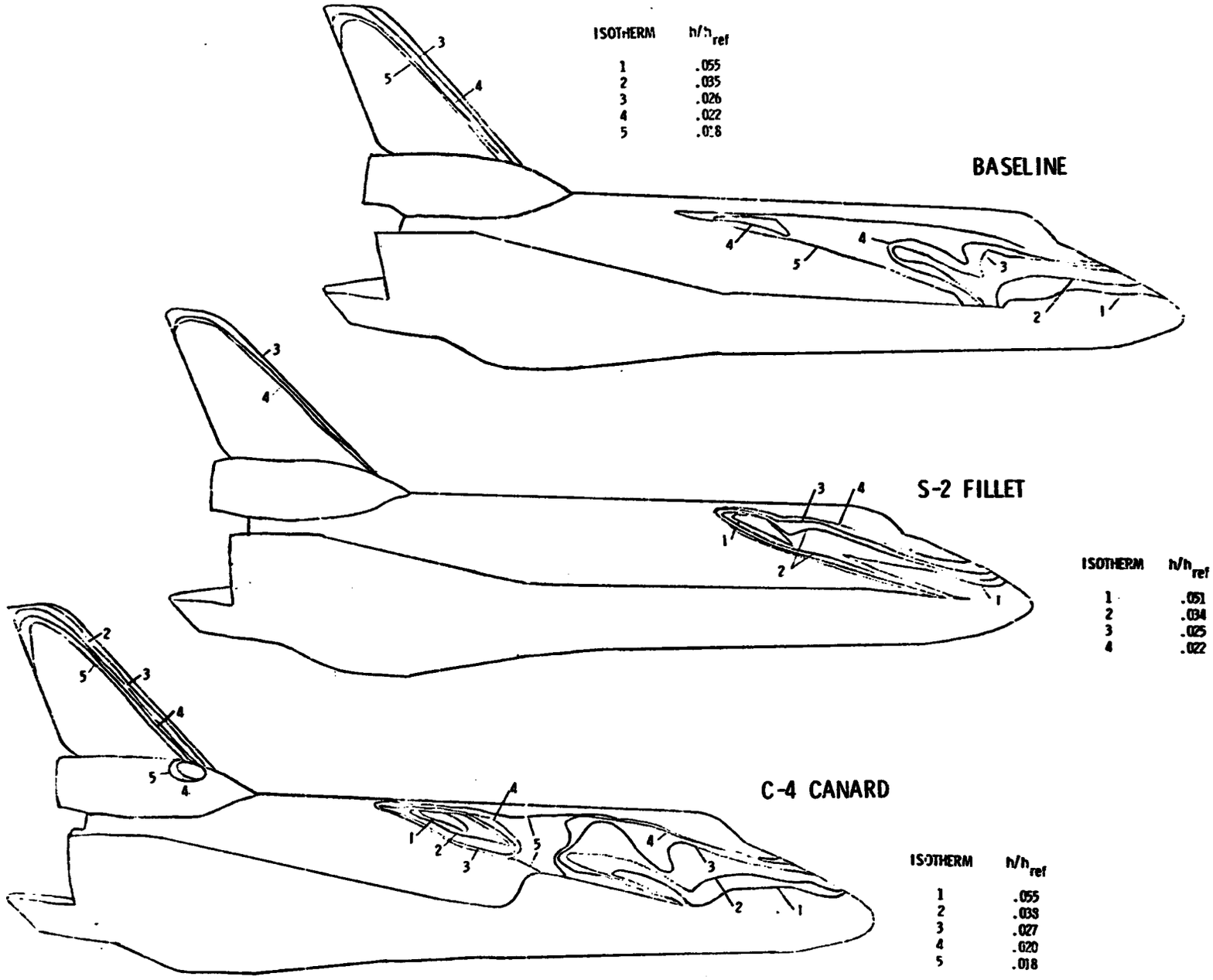

(c) $\alpha = 40^0$. $Re_L = 10^6$

Figure 8. - Concluded.

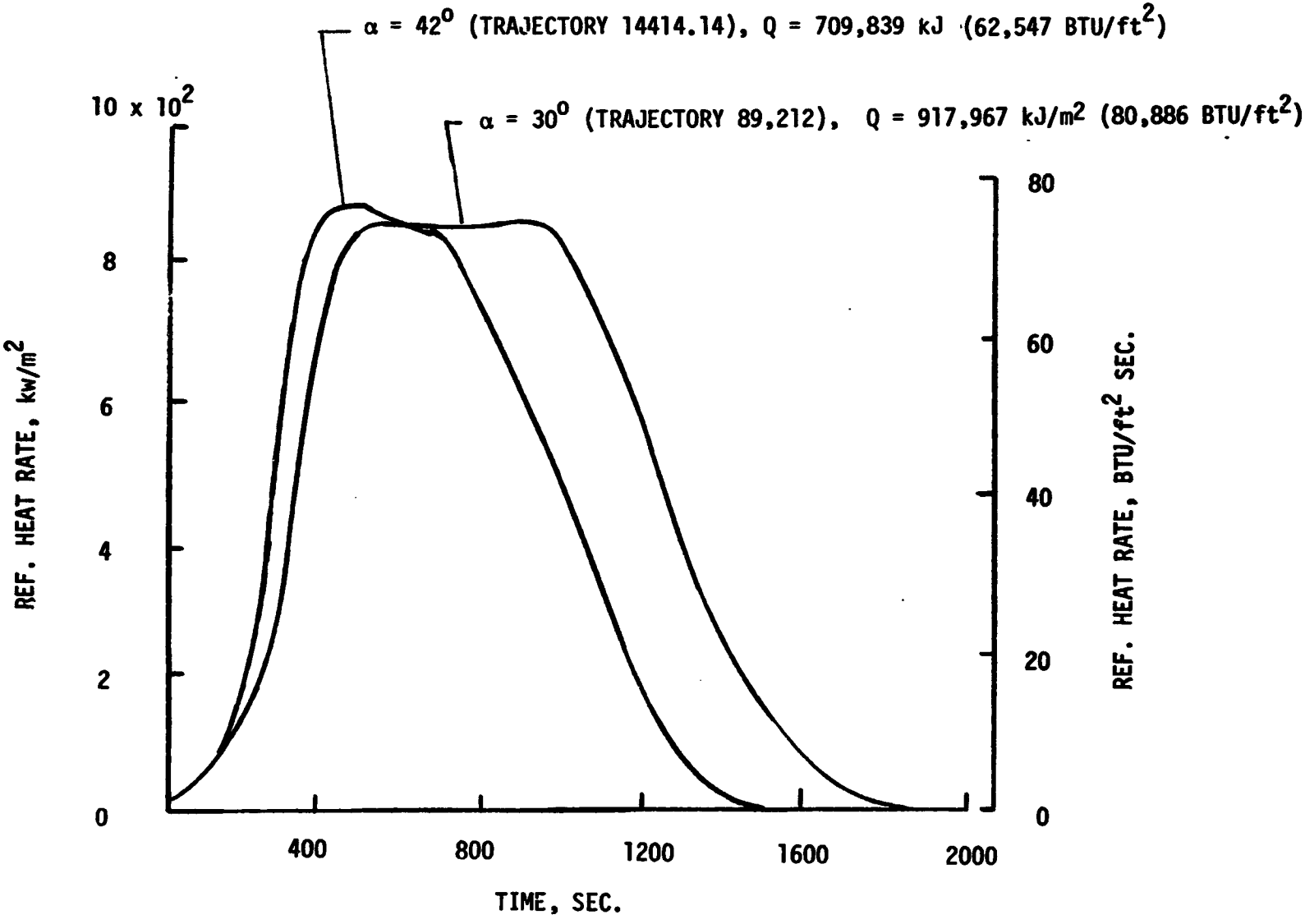

Figure 9.- Reference sphere (r = 0.3048 m (1 ft)) heating rate for reentry times from 122,000 m (400,000 ft) altitude.

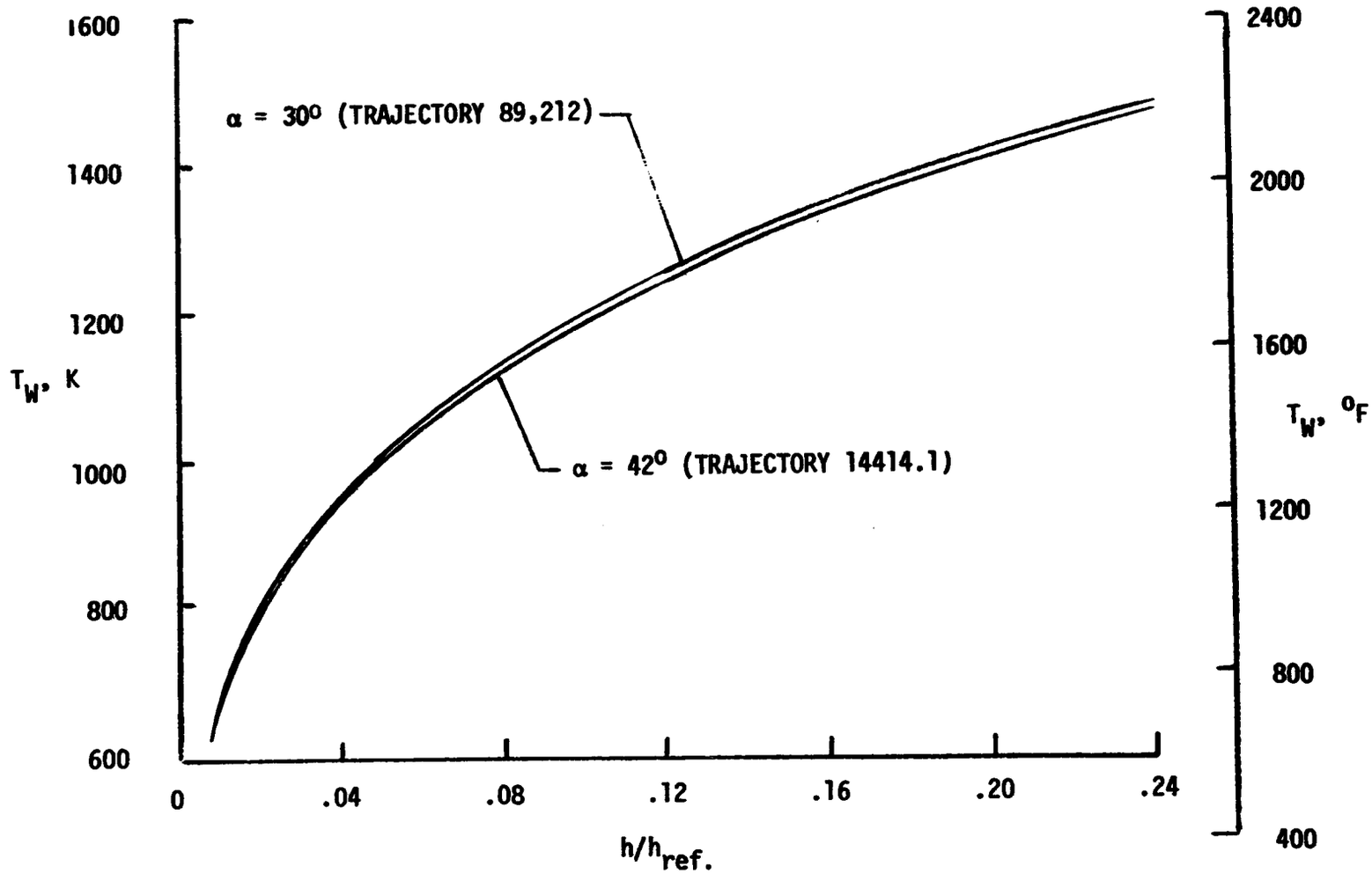

Figure 10.- Radiation equilibrium temperature for heating-rate ratio. $\varepsilon = 0.8$.

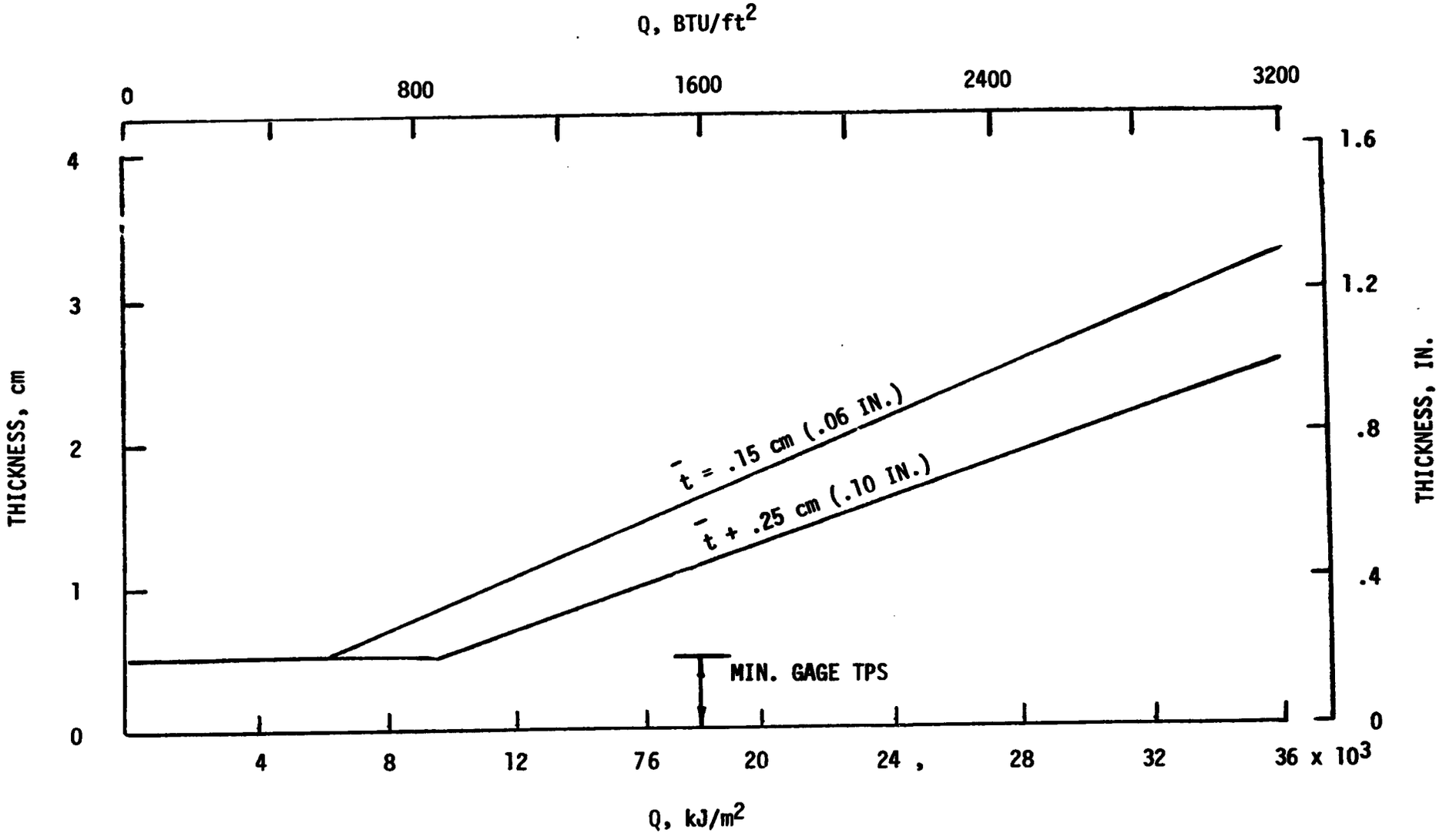

Figure 11.- RSI thickness for maximum backface temperature of 424K (350°F) for various heat loads.

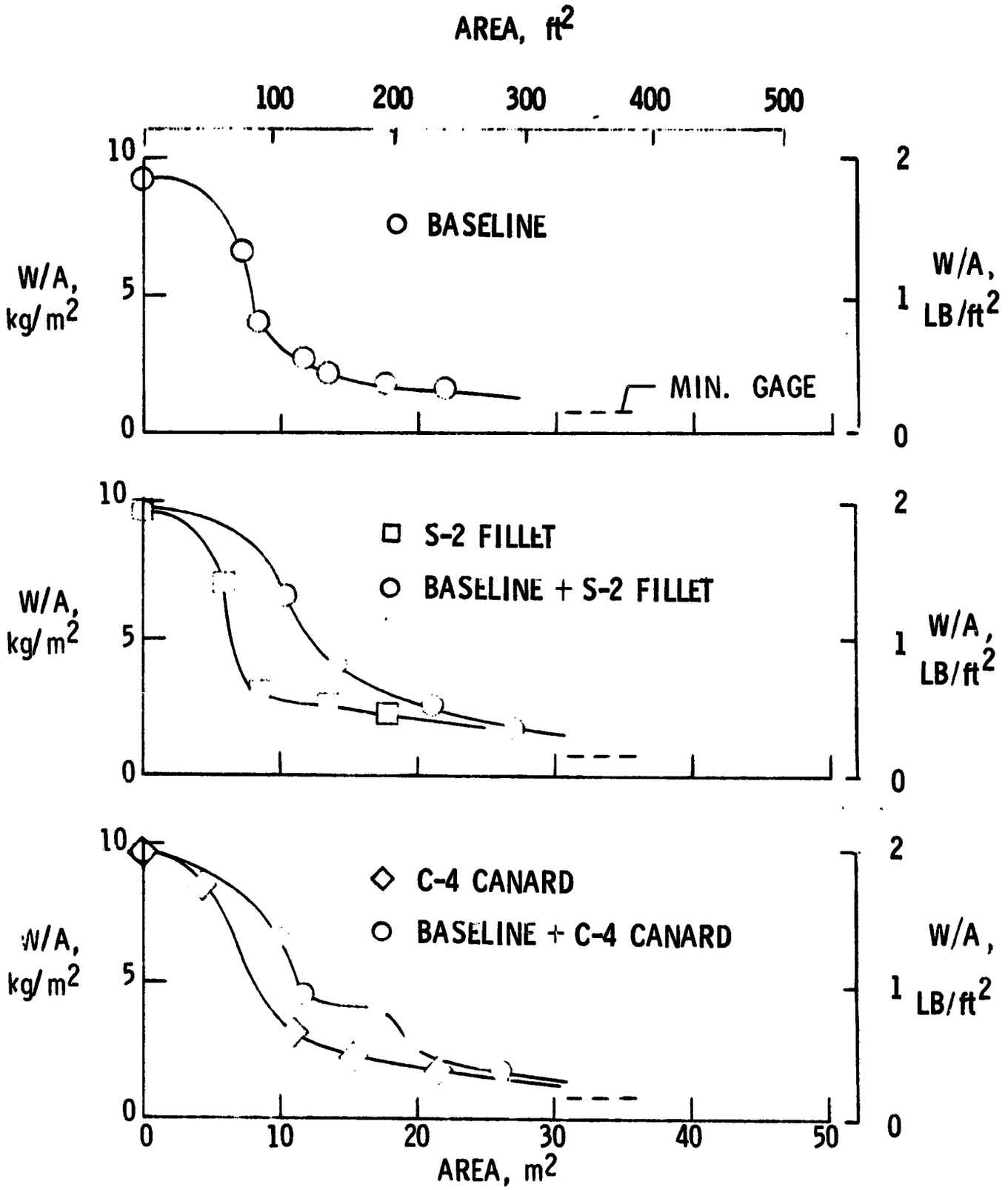

(a) $\alpha = 30°$; $Re_L = 1 \times 10^6$

Figure 12.- Unit weights of TPS required for areas on one side of shuttle orbiter configurations.

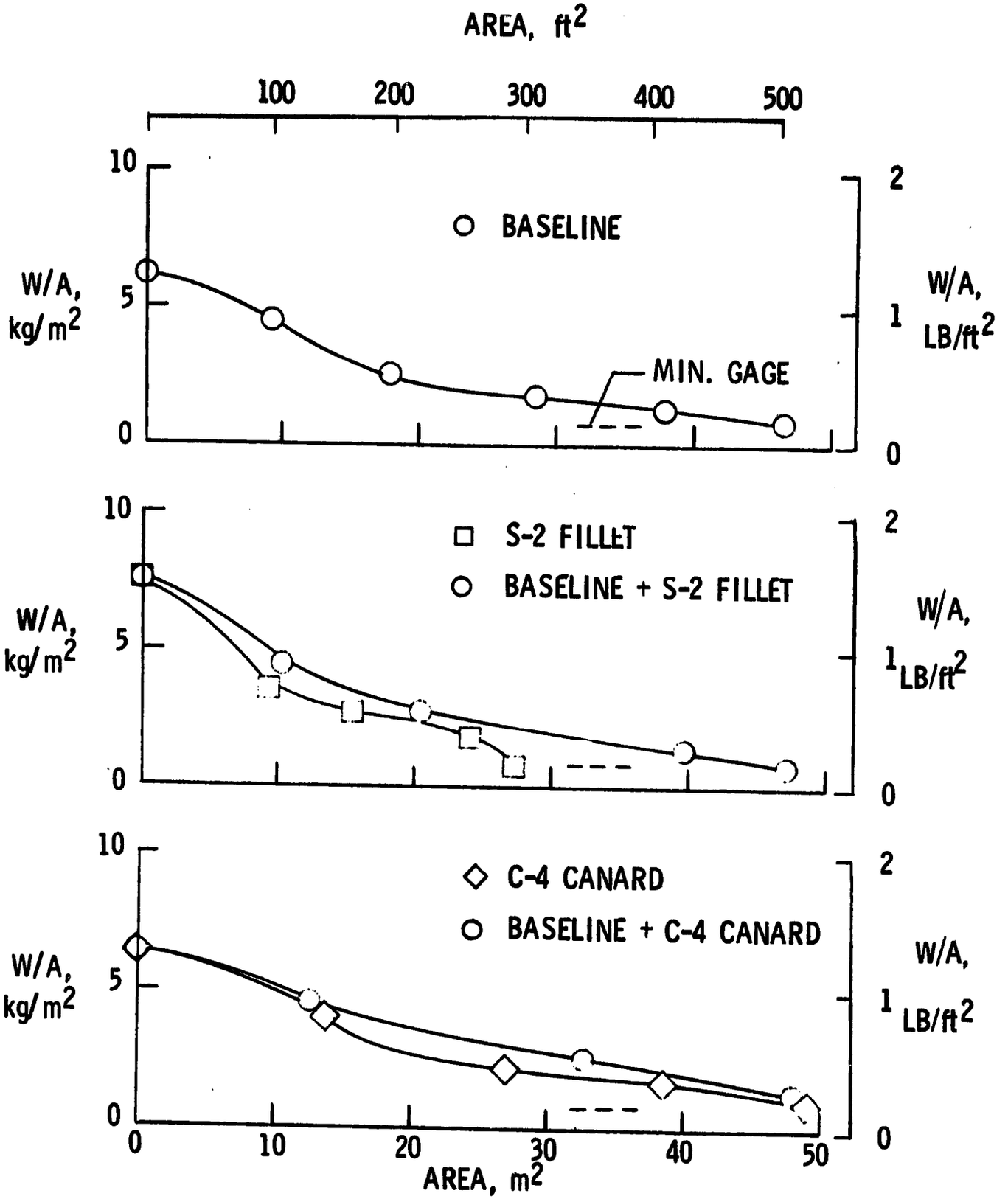

(b) $\alpha = 30°$; $Re_L = 2 \times 10^6$

Figure 12.- Continued

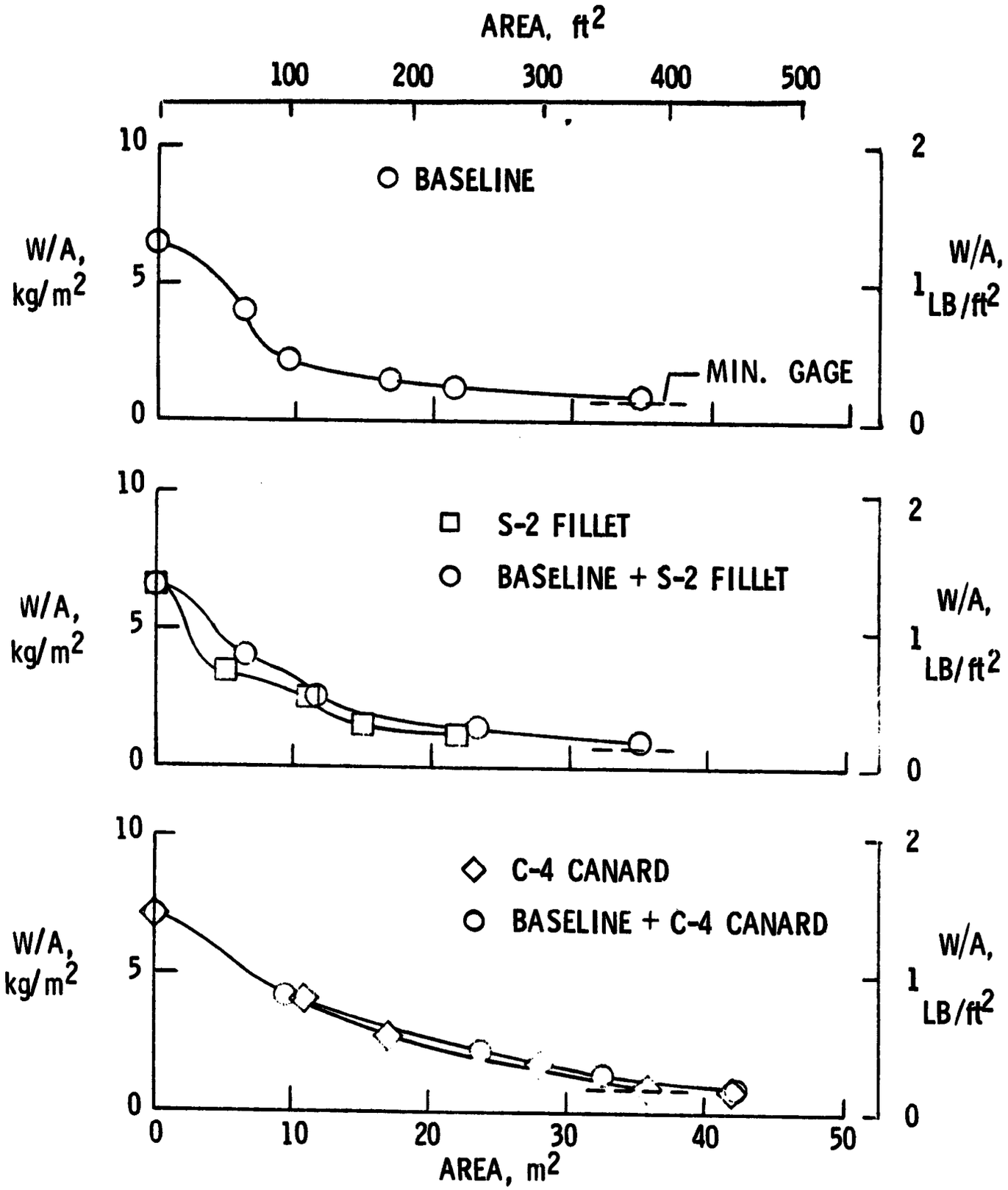

(c) $\alpha = 40°$; $Re_L = 1 \times 10^6$

Figure 12.- Concluded